

Wave Breaking Events and their link to Rossby Wave Packets and Atmospheric Blockings during Southern Hemisphere Summer

Iago Perez¹, Marcelo Barreiro Parrillo¹, Noemie Ehstand², Emilio Hernández-García³, and Cristóbal López⁴

¹Universidad de la República

², Instituto de Física Interdisciplinar y Sistemas Complejos

³IFISC (CSIC-UIB), Instituto de Física Interdisciplinar y Sistemas Complejos

⁴Instituto de Física Interdisciplinar y Sistemas Complejos (UIB-CSIC)

December 20, 2022

Abstract

Rossby Wave packets (RWPs) are atmospheric perturbations located at upper levels in mid-latitudes which, in certain cases, terminate in Rossby Wave Breaking (RWB) events. When sufficiently persistent and spatially extended, these RWB events are synoptically identical to atmospheric blockings, which are linked to heatwaves and droughts. Thus, studying RWB events after RWPs propagation and their link with blocking is key to enhance extreme weather events detection 10-30 days in advance. Hence, here we assess (i) the occurrence of RWB events after the propagation of RWPs, (ii) whether long-lived RWPs (RWPs with a lifespan above 8 days, or LLRWPs) are linked to large-scale RWB events that could form a blocking event, and (iii) the proportion of blocking situations that occur near RWB events. To do so, we applied a tracking algorithm to detect RWPs in the Southern Hemisphere during summertime between 1979-2020, developed a wave breaking algorithm to identify RWB events, and searched for blocking events with different intensities. Results show that LLRWPs and the other RWPs displayed large-scale RWB events around 40% of the time, and most RWB events in both distributions last around 1-2 days, which is not long enough to identify them as blocking situations. Nearly 17% of blockings have a RWB event nearby, but barely 5% of blockings are linked to RWPs, suggesting that propagating RWPs are not strongly linked to blocking development. Lastly, large-scale RWB events associated with RWPs that lasted less than 8 days are influenced by the Southern Annular Mode and El Niño-Southern Oscillation.

1
2 **Wave Breaking Events and their link to Rossby Wave Packets and Atmospheric**
3 **Blockings during Southern Hemisphere Summer**
4

5 Iago Pérez-Fernández¹, Marcelo Barreiro¹, Noémie Ehstand², Emilio Hernández-García²,
6 Cristobal López².

7 ¹*Departamento de Ciencias de la atmósfera y Física de los Océanos, Facultad de Ciencias, Universidad de la*
8 *República, Montevideo, Uruguay.*

9 ²*Instituto de Física Interdisciplinar y Sistemas Complejos (IFISC), CSIC-UIB. Palma de Mallorca, Spain.*

10 Corresponding author: Iago Pérez-Fernández (iperez@fisica.edu.uy)

11 **Key Points:**

- 12 • Large-scale wave breaking events caused by propagating Rossby Wave Packets do not
13 usually last enough to develop into an atmospheric block.
- 14 • Years with La Niña and positive Southern Annular Mode favor large-scale wave breaking
15 activity linked to short-lived Rossby Wave packets.
- 16 • Near 17% of blocking events appear preceded by a wave breaking event but most of them
17 are not linked to propagating Rossby Wave Packets.

18 **Abstract**

19 Rossby Wave packets (RWPs) are atmospheric perturbations located at upper levels in mid-latitudes which, in certain cases,
 20 terminate in Rossby Wave Breaking (RWB) events. When sufficiently persistent and spatially extended, these RWB events are
 21 synoptically identical to atmospheric blockings, which are linked to heatwaves and droughts. Thus, studying RWB events after
 22 RWPs propagation and their link with blocking is key to enhance extreme weather events detection 10-30 days in advance.
 23 Hence, here we assess (i) the occurrence of RWB events after the propagation of RWPs, (ii) whether long-lived RWPs (RWPs
 24 with a lifespan above 8 days, or LLRWPs) are linked to large-scale RWB events that could form a blocking event, and (iii) the
 25 proportion of blocking situations that occur near RWB events. To do so, we applied a tracking algorithm to detect RWPs in the
 26 Southern Hemisphere during summertime between 1979-2020, developed a wave breaking algorithm to identify RWB events,
 27 and searched for blocking events with different intensities. Results show that LLRWPs and the other RWPs displayed large-scale
 28 RWB events around 40% of the time, and most RWB events in both distributions last around 1-2 days, which is not long enough
 29 to identify them as blocking situations. Nearly 17% of blockings have a RWB event nearby, but barely 5% of blockings are
 30 linked to RWPs, suggesting that propagating RWPs are not strongly linked to blocking development. Lastly, large-scale RWB
 31 events associated with RWPs that lasted less than 8 days are influenced by the Southern Annular Mode and El Niño-Southern
 32 Oscillation.

33 **Plain Language Summary**

34 When an atmospheric wave breaks in the upper level of the atmosphere, it modifies the wind flow and local weather conditions.
 35 If these wave breaking events are sufficiently big and stable, they can produce atmospheric blocking events, which are linked to
 36 heatwaves and drought development. In this study, we assess if a link between wave breaking events caused by long-lived
 37 traveling atmospheric waves (atmospheric waves that last more than 8 days in the atmosphere) and blocking events development
 38 exists during Southern hemisphere summer. Independently of the duration of the wave packets, near 4 out of 10 times they cause
 39 very extensive wave breaking events, but they do not last long enough to be considered an atmospheric blocking. Oppositely,
 40 nearly 20% of blocking events manifest nearby a wave breaking event independently of the strength of the block, but these wave
 41 breaking events do not seem to be linked to traveling wave packets. Therefore, this study suggests that traveling atmospheric
 42 waves are not directly related to the development of atmospheric blockings. Also, the occurrence of extensive wave breaking
 43 events caused by traveling atmospheric waves that last less than 8 days are affected by phenomena like El Niño or the Southern
 44 Annular Mode.

45 **Keywords** — Rossby Wave Packets, Wave Breaking, ENSO, SAM, Atmospheric Blocking

46 **1 Introduction**

47 Rossby Wave Packets (RWPs) are synoptic scale perturbations that appear in the upper
 48 atmosphere of mid-latitudes. During their propagation, these packets travel by downstream
 49 development mechanisms, transporting large quantities of energy in the process (Tu-Cheng Yeh
 50 1949, Chang and Yu 1999; Chang 2000). RWPs play an important role in the global atmospheric
 51 circulation because they are related to storm track variability (Souders *et al.*, 2014a). In addition,
 52 they are precursors of extreme weather events such as heatwaves, extreme rainfall (Chang 2005;
 53 Grazzini and Vitart 2015, O'brien and Reeder 2017, Wirth *et al.*, 2018) and extratropical cyclone
 54 development (Chang *et al.*, 2005, Sagarra and Barreiro 2020). Also, during their propagation
 55 they increase the uncertainty of middle-long range forecast (from 3 to >10 days in advance) in
 56 the areas they cross (Zheng *et al.*, 2013). Normally, these packets tend to last between 3-6 days
 57 in the atmosphere but, under certain circumstances, they can last up to 2-3 weeks before
 58 disappearing (e.g. Pérez *et al.*, 2021). When RWPs have a lifespan longer than 8 days, they are
 59 referred to as long-lived RWPs or LLRWPs (Grazzini and Vitart 2015).

60 The lifespan and propagation of the RWPs greatly depend on the potential vorticity gradients and
 61 the locations of diabatic heating sources (Grazzini and Vitart 2015). Potential vorticity gradients
 62 shape the waveguide where the RWPs propagate, such that a very zonal and intense jet with

63 narrow potential vorticity gradients favor the development of very stable RWPs (Chang & Yu
64 1999, Souders *et al.*, 2014b, Wirth *et al.*, 2020), whereas weaker gradients damp or stop the
65 wave packets propagation (Grazzini and Vitart 2015).

66 Due to the lack of large baroclinically unfavorable areas in the Southern Hemisphere, RWPs are
67 easier to detect than in the Northern Hemisphere (Grazzini and Vitart 2015). In addition, during
68 austral summer (December to March) the jet stream displays a very zonal and narrow wind flow,
69 which acts as a waveguide where RWPs propagate (Hoskins & Ambrizzi, 1993; Chang, 1999),
70 and facilitates RWPs detection. Pérez *et al.*, (2021) showed that the Southern Annular Mode
71 (SAM) heavily influences the development of LLRWPs during austral summer, such that years
72 with positive SAM disfavor LLRWPs development whereas negative SAM favor them.
73 Conversely, El Niño-Southern Oscillation (ENSO) influence was found to be less robust.

74 When RWPs reach the end of their life cycle they can “break”, causing an irreversible mixing of
75 potential vorticity fields over a longitudinally confined region (Simmons and Hoskins 1978,
76 McIntyre and Palmer 1983, 1984). As a result, high potential vorticity air intrudes the
77 troposphere and/or low potential vorticity air enters in the stratosphere, causing the development
78 of potential vorticity anomalies that can either remove or reverse the usual potential vorticity
79 meridional gradients. This process is called Rossby Wave Breaking or RWB (McIntyre and
80 Palmer 1983, 1984, Berrisford *et al.*, 2007, Masato *et al.*, 2011). RWB events are key to the air
81 mass exchange between the troposphere and the stratosphere (Holton *et al.*, 1995), and are
82 considered as potential precursors of weather regime transitions (Michel and Rivière 2011) that
83 can increase the prediction skill of precipitation (Ryo *et al.*, 2013). In addition, RWB events
84 share some characteristics with atmospheric blocking. In fact, RWB events that show a spatial
85 and temporal scale similar to atmospheric blocking are synoptically recognized as a blocking
86 (Berrisford *et al.*, 2007). An atmospheric blocking event is a nearly-stationary large-scale pattern
87 in the pressure field arising from the reversal of the westerly wind flow, and it is stable enough to
88 last from several days to weeks in the atmosphere (Rex, 1950, Patterson *et al.*, 2019). Its
89 appearance is linked to the development of extreme weather events such as heatwaves or
90 droughts (Woollings, *et al.*, 2018). Nonetheless, even if we find some RWB events prior to the
91 onset of some atmospheric blockings (Altenhoff *et al.*, 2008), not all events are associated with
92 blocking (Hitchman and Huesmann 2007, Masato *et al.*, 2013).

93 There are two main types of RWB (Thorncroft *et al.*, 1993), one is cyclonic RWB, where low
94 potential temperature or “cold” air from the dynamical tropopause moves eastward and
95 equatorward to the west of high potential temperature air or “warm” air, whereas “warm” air
96 goes poleward and westward. The other is anticyclonic RWB, where the equatorward and
97 westward movement of low potential temperature air is to the east of the poleward and eastward
98 movement of the “warm” air. Each morphology of wave breaking implies different changes in
99 synoptic circulation. Anticyclonic RWB occurs with much more frequency than cyclonic RWB

100 because RWPs propagating in the tropopause tend to break in an anticyclonic fashion
101 (Thorncroft *et al.*, 1993; Peters and Waugh 1996, 2003).

102 Several studies of RWB were done for the Northern Hemisphere (e.g. Strong and Magnusdottir
103 2008, Masato *et al.*, 2011, Michel and Rivière 2011, Ryoo *et al.*, 2013). For example, Thorncroft
104 *et al.* (1993) found that RWB frequency is influenced by processes that alter the wind flow. In
105 that regard, Strong and Magnusdottir (2008) concluded that the positive phase of the Northern
106 Annular Mode is associated with anticyclonic RWB, whereas its negative phase is linked to
107 cyclonic RWB. In the Southern Hemisphere, Berrisford *et al.*, (2007) showed that RWB in mid
108 latitudes wintertime is concentrated in the east Pacific, whereas during summertime RWB
109 episodes are less frequent and are confined to the west Pacific. This is in (qualitative) agreement
110 with the observed location of Southern hemisphere blocking. Gong *et al.*, (2010) studied the
111 influence of SAM and ENSO on RWB breaking during austral spring-summer, and found that
112 the positive phase of SAM shows higher wave breaking activity than the negative. Additionally,
113 Wang and Magnusdottir (2010) observed that anticyclonic and cyclonic RWB frequency is
114 affected by the changes in background flow caused by ENSO events.

115 A question still unanswered is the relationship between the occurrence of RWB and the
116 propagation of RWPs in the Southern hemisphere, as well as whether RWPs can cause RWB
117 events that can trigger atmospheric blocking development. Thus, the aim of this research is to
118 study the detection and evolution of RWB events after the propagation of transient RWPs, with
119 special emphasis on large-scale RWB. In addition, we classified the RWB considering whether
120 their associated RWPs is a LLRWPs or not. This is done in order to assess whether the wave
121 breaking events caused by LLRWPs share different characteristics as the those found for the rest
122 of the RWPs, and study whether RWB events that occur after the dissipation of a LLRWPs are
123 linked to the development of atmospheric blocking.

124 The paper is organized as follows. Section 2 describes the datasets and the methodologies for
125 tracking RWPs, detecting RWB events, as well as blockings. Section 3 focuses on the link
126 between RWB and RWPs, section 4 on the interannual variability of RWB events and the
127 potential impact of global climate modes, and section 5 assesses the link between atmospheric
128 blocking and RWB events. Finally, section 6 presents a summary of the study.

129 **2 Data and methodology**

130 2.1 Data

131 In this study, we used ERA 5 Reanalysis (Hans *et al.*, 2020), with an horizontal resolution of
132 $0.25^\circ \times 0.25^\circ$ and daily frequency. The region of study consists of the mid-latitudes of the
133 Southern Hemisphere, during austral summer (December to March or December-March)
134 between 1979-2021 as done in previous studies (Sagarra and Barreiro 2020, Pérez *et al.*, 2021).
135 Thus, we have 41 seasons available for the analysis.

136 RWPs propagate in the upper atmosphere of mid-latitudes and manifest as meanders of the jet
137 stream. During their propagation, they produce a series of troughs and ridges that travel confined
138 to a certain latitudinal band, moving mainly eastward during austral summer (Chang 1999).
139 Thus, by computing the envelope of the meridional wind speed at 300 hPa ($V_{300\text{env}}$), we can
140 characterize these transient RWPs. To calculate the $V_{300\text{env}}$, we followed the methodology
141 specified in Pérez *et al.*, (2021). Next, due to the fact that RWPs propagation is mostly zonal
142 during December-March season (Chang 1999), we averaged the $V_{300\text{env}}$ data between the
143 latitudinal range of 40-65°S.

144 Regarding the detection of RWB events, as in previous studies, we have used the potential
145 vorticity field in isentropic coordinates, searching for areas where the usual meridional potential
146 vorticity gradient either disappears or is inverted. The computation of the potential vorticity field
147 was performed following Hoskins *et al.*, (1985), using daily temperature and wind speed at 300
148 hPa interpolated to the isentropic coordinates of 330°K.

149 Also, to characterize the interannual variability and amplitude of the global climate modes, we
150 used the Oceanic Niño Index for ENSO, and the Antarctic Oscillation index for SAM. Both
151 datasets are publicly available in the NOAA website (<https://origin.cpc.ncep.noaa.gov/>).

152 2.2 Description of Rossby Wave Packet tracking algorithm

153 The RWPs are detected using a tracking algorithm, based on the maximum envelope technique
154 (Grazzini and Vitart 2015, Sagarra and Barreiro 2020, Pérez *et al.*, 2021). This algorithm
155 searches for areas with the highest daily values of $V_{300\text{env}}$, identifying the center of activity of the
156 RWPs, and then follow the propagation of the wave packets to the east, assuming that they travel
157 between 15-45°E per day. Before applying the tracking algorithm, we filter out small values of
158 $V_{300\text{env}}$ to avoid tracking noise. Although there is no optimum threshold because there are no
159 physical properties that separate one wave packet from another (Souders *et al.*, 2014b), here we
160 applied a minimum threshold of 19 m/s. Pérez *et al.*, (2021) show that the tracking of RWPs is
161 not sensitive to the choice of threshold between 17-21 m/s.

162 It is also worth pointing out that the tracking algorithm only follows transient RWPs that is,
163 RWPs that propagate eastwards and have a zonal wavenumber between 4-11, which corresponds
164 to the transient structures of the Southern Hemisphere (Trenberth 1981). Therefore, the algorithm
165 cannot track stationary RWPs, or those RWPs with a wavenumber ≤ 3 . Hereafter, when we talk
166 about RWPs, we are referring to these transient RWPs.

167 After the algorithm finishes tracking all the RWPs of the season, it uses proximity criteria to link
168 trajectories of the RWPs that were interrupted, and then measures the characteristics of the
169 tracked wave packet: longitudinal extension, areas of formation/dissipation, lifespan and
170 propagation speed. The full description of the algorithm is available in Pérez *et al.*, (2021).

171 Finally, for the subsequent analysis, the tracked RWPs are classified in LLRWPs (lifetime >8
172 days) and short lived RWPs or SLRWPs (lifetime ≤ 8 days).

173 2.3 Rossby Wave Breaking detection algorithm and validation

174 As we mentioned in section 2.1, RWB events manifest in the upper atmosphere in areas where
175 the usual meridional gradient of potential vorticity either disappears or reverses. We can detect
176 these areas by locating where the potential vorticity contour lines overturn following isentropic
177 coordinates (McIntyre and Palmer 1983). Previous studies in the Southern Hemisphere followed
178 potential vorticity contours in the isolines between 310-350°K (Ndarana and Waugh 2010 a, b,
179 Strong and Magnusdottir 2008) because they represent the dynamical tropopause between the
180 high latitudes and the subtropics (Ndarana and Waugh 2010 a).

181 We choose to study RWB events that occur in the potential vorticity of -2 PVU (1 PVU = 10^{-6}
182 $\text{m}^2 \text{s}^{-1} \text{K kg}^{-1}$) on the 330°K isosurface. The reason to chose this specific isosurface is because it
183 is a transitional region between the isosurface 310-350°K, where anticyclonic and cyclonic shear
184 have been found (Ndarana and Waugh 2010 a, b).

185 In order to identify RWB events we developed an objective algorithm based on the methodology
186 of Barnes and Hartmann (2012). The steps of the algorithm are the following:

187 1.- Representation of the -2 PVU contour line for day t , and retention of the longest contour line.
188 This is done to avoid the detection of isolated potential vorticity “bubbles” as part of RWB
189 events.

190 2.- Identification of areas where -2 PVU contours crosses more than 2 times the same
191 longitudinal section. These points are referred as wave breaking points.

192 3.- If there are wave breaking points closer than 500 km from each other we assumed that these
193 points belong to the same wave breaking event (Barnes and Hartmann 2012).

194 4.- Retention of RWB events that have a longitudinal extension $\geq 5^\circ$. This avoids registering
195 meridionally extended potential vorticity tongues that do not show overturning.

196 5.- Classification of the RWB event regarding their orientation. This is done by measuring the
197 latitudinal mean of the 4 most eastward and westward overturning points of the RWB episode. In
198 the Southern Hemisphere, cyclonic RWB events have their western-most overturning point
199 located equatorward, while their east-most overturning point is poleward. By contrast, in
200 anticyclonic RWB events their eastern-most overturning point are equatorward whereas their
201 west-most overturning point are poleward. Thus, if the latitudinal mean of their most westward
202 points of the contour is closer to poleward latitudes than the observed at the most eastward
203 points, we assume that the wave packet shows an anticyclonic shear, whereas if the most
204 westward points are closer to the equator than the most eastward points, the breaking event is

205 classified as cyclonic RWB. An example of the application of the RWB tracking algorithm can
206 be seen in figure 1.

207 6.- Measurement of the RWB characteristics: longitudinal and latitudinal extension of the event,
208 day of detection, and type of RWB shear.

209 7.- Repeat steps 1-6 for the following days until all the data is analyzed.

210 Given the few studies reported on RWB for the Southern hemisphere it is important first to
211 ensure that the detection algorithm works as expected. To do so, we first tracked wave breaking
212 events in the December-March season only between 1979-2008, and compared our results
213 against previous studies (Ndarana and Waugh 2010 a,b, Wang and Magnusdottir 2010).

214 2.4 Linking large-scale Rossby wave breaking events to Rossby Wave Packets

215 In this section we explain the methodology used to link RWB activity to the dissipation of
216 RWPs. At the moment of writing this article, the authors were not able to find a study which
217 links RWB events with RWPs in the Southern Hemisphere.

218 Before describing the methodology, it is important to highlight that in this section we will only
219 consider large-scale RWB, that is RWB events with a longitudinal extension of 1000 km ($\sim 15^\circ$ in
220 mid latitudes) or above (Barnes and Hartmann 2012). This is done in order to retain wave
221 breaking events that can strongly affect the large-scale atmospheric circulation and have a spatial
222 scale similar to atmosphere blocking, (11° of extension, Patterson *et al.*, 2019).

223 The methodology used for linking RWPs with RWB events has the following steps:

224 1.-Apply the RWB tracking algorithm at day T_f , being T_f the day when a RWP finished its
225 propagation.

226 2.-If the algorithm detects the beginning of a RWB event located between $X_f \pm 2000$ km, being
227 X_f the longitudinal section where the algorithm located a RWPs before stopping its propagation,
228 we assume that the wave breaking event registered is linked to the RWP that stopped its
229 propagation and we proceed to step 3. If the described condition is not fulfilled, we continue
230 looking for RWB events for the following days. If by day T_{f+4} we do not find a RWB event that
231 matches the described condition, we assumed that the RWP did not show a RWB episode and
232 finish the search. Oppositely, if after applying the wave breaking detection algorithm we detect
233 two or more RWB event which are in the range $X_f \pm 2000$ km, we select the RWB whose
234 geographical center is closer to the area of dissipation of the RWP.

235 3.-We register the day when a RWB event is detected as T_n , and applied the RWB tracking
236 algorithm at day T_{n+1} . If a RWB event exists with geographical center within 20° (~ 1400 km) of
237 distance or less from the wave breaking episode found at day T_n , we assume that this event is an

238 extension of the RWB event found the previous day. Else, we infer that the RWB episode only
239 lasted for a day.

240 4.- Step 3 is repeated for the following days until we stop finding wave breaking events that
241 fulfill the condition specified in step 2.

242 5.- We save the same characteristics of the RWB events detailed in section 2.3 as well as the day
243 a RWB event was detected after the dissipation of a RWP, and how many days lasts the RWB
244 associated to a RWP.

245 In step 2, we search for RWB events in the area located between $X_f \pm 2000$ km because even if
246 X_f signals the center of the RWP, the packet has a certain longitudinal extension, and thus the
247 RWB event does not have to necessarily appear near X_f . Barnes and Hartmann (2012) considered
248 that RWB events that are within 2000 km of the geographical center of the RWB belong to the
249 same episode, hence, in this study we look for RWB events that are up to 2000 km of distance
250 from the area of dissipation of the RWPs. On the other hand, we chose to search for events a few
251 days after the end of the RWPs propagation because it is possible that before disappearing the
252 RWPs might be stationary for a few days. By examining the evolution and behavior of several
253 potential vorticity fields several days after the dissipation of a RWPs we chose an upper limit of
254 4 days.

255 Additionally, in step 3 we used a distance of 1400 km to search for the continuation of a RWB
256 episode, because using a longer distance can cause the algorithm to select a wrong wave
257 breaking event that is too far away from the original episode that is being tracked.

258 Figure 2 shows an example of the methodology followed to link RWPs with RWB events.

259 2.5 Linking atmospheric blocking to large-scale Rossby wave breaking events

260 Lastly, we compared the proportion of large-scale RWB events that are present nearby the
261 development of an atmospheric blocking event. In order to detect the occurrence of atmospheric
262 blocking events, we use the methodology of Tibaldi and Moldenti (1989), but modified to
263 consider a range of latitudes in the Southern Hemisphere following Mendes *et al.*, (2011). This
264 technique measures two geopotential height meridional gradients from a central latitude, one to
265 the north (GHGN) and another one to the south (GHGS) by using expressions 1 and 2.

$$266 \quad (1) \text{ GHGN} = (Z(\lambda, \theta_1) - Z(\lambda, \theta_N)) / (|\theta_1 - \theta_N|)$$

$$267 \quad (2) \text{ GHGS} = (Z(\lambda, \theta_S) - Z(\lambda, \theta_2)) / (|\theta_S - \theta_2|)$$

268 Where

$$269 \quad \theta_N = 40^\circ\text{S} + \Delta$$

$$270 \quad \theta_2 = 50^\circ\text{S} + \Delta$$

271 $\theta_1 = 55^\circ\text{S} + \Delta$

272 $\theta_s = 65^\circ\text{S} + \Delta$

273 $Z(\lambda, \theta)$ is the geopotential height at 500 hPa in a latitude θ and longitude λ , and Δ belongs to the
274 set $\{-10, -7.5, -5, -2.5, 0, 2.5, 5, 7.5, 10\}$. If on a specific day, at a given longitude λ ,
275 $\text{GHGN} > 0$ and $\text{GHGS} < -10$ m/degree of latitude for, at least, one value of Δ , the longitude is
276 considered to be “blocked”. Note that, we measure GHGN and GHGS using slightly different
277 expressions from Mendes *et al.*, (2011). The definition chosen here implies a stronger
278 requirement on the blocked longitudes than the one considered in the latter study.

279 Once instantaneous, local, blocked conditions have been identified, additional persistence and
280 spatial extension requirements must be imposed to define atmospheric blocking events. Various
281 thresholds have been used in the literature. Patterson *et al.*, (2019) define an atmospheric
282 blocking event when they detect a blocked longitudinal sector covering, at least, 11° and when
283 this condition persists for a minimum of 4 days in the atmosphere. Mendes *et al.*, (2011), use a
284 minimum spatial extent of 7.5° in longitude and persistence of 5 days. In our study, we registered
285 events that have a minimum longitudinal extension of $7.5, 10, 12.5$ and 15° and display a
286 minimum lifespan of 4-5 days, measuring the longitude of detection, lifetime and zonal
287 extension of the blocks. This is done in order to assess whether the proportion of atmospheric
288 blocks that might be linked to RWB is sensitive to the blocking conditions. Hence, events that
289 last at least 4 days with a longitudinal extension of 7.5° are most frequent and represent blocking-
290 like situations, that is, the persistent reversal of the westerly wind flow that are not sufficiently
291 extensive to be considered as a blocking event, whereas those that last more than 5 days and have
292 a zonal extension of at least 15° are considered the strongest blocks of the dataset.

293 In section 5, we first verify that our algorithm works as intended by measuring the frequency of
294 occurrence and areas of formation of blocking events in our period of study, comparing the
295 results to those obtained in Mendes *et al.*, (2011). We then study the potential links between
296 large-scale RWB events and blocking events by identifying the events which occur on the same
297 day and such that their respective geographical center are separated by a maximum of 2000 km.
298 The fulfillment of the latter conditions ensures that the RWB event is present near the
299 development of the atmospheric block. Lastly, we determine how many of the RWB events that
300 occur near an atmospheric block are associated to propagating RWPs. This analysis assesses the
301 proportion of atmospheric blocks that are associated to large-scale RWB activity, and whether
302 RWB activity linked to propagating RWPs is directly linked to the development of atmospheric
303 blocking events.

304 **3 Rossby wave breaking events and their relationship to Rossby Wave Packets**

305 3.1 Verification of Rossby Wave Breaking algorithm

306 The analysis of RWB events during the December-March season between 1979-2008 detected a
307 total of 659 RWB events in December, 470 in January, 413 in February and 581 events in March.
308 As for the orientation of the RWB events, 22% of the total wave breaking activity belongs to
309 cyclonic RWB, and the rest to anticyclonic RWB.

310 Figure 3 shows the longitudinal distribution of RWB frequency of occurrence. The maximum
311 RWB activity occurs in the western Pacific (between 140-200° E), and the lowest activity is
312 located near 0°E. These results indicate that RWB is weakest at the jet entrance in the Atlantic
313 basin, and largest at the jet exit, consistent with the fact that RWPs activity occurs in the
314 Atlantic-Indian basin where the strong jet acts as waveguide (Pérez *et al.*, 2021).

315 Additionally, figure 4 shows that the main area of anticyclonic RWB detection is located in the
316 western Pacific, as reported by Ndarana and Waugh (2010b). Nonetheless, we also observe two
317 secondary areas of maximum anticyclonic RWB activity, one located in the Indian Ocean and
318 the second in the eastern Pacific-western Atlantic. The latter is in agreement with Ndarana and
319 Waugh (2010b), but these authors found very little anticyclonic RWB activity in the Indian
320 Ocean during December-February. Nonetheless, Ndarana and Waugh (2010b) found significant
321 RWB activity in that region during March-May, suggesting that the differences with our results
322 are explained because of our consideration of March in the summer season. Thus, overall our
323 results are close to those observed in Ndarana and Waugh (2010b), providing a verification of
324 our RWB algorithm. It is worth pointing out that in our case the areas of RWB frequency have
325 wider meridional extension than those found in Ndarana and Waugh (2010b), because our
326 algorithm registers the whole latitudinal area where the overturning potential vorticity is
327 detected.

328 3.2 Characteristics of Rossby Wave Breaking after Rossby Wave Packet propagation

329 For the Southern Hemisphere summertime during 1979-2021, a total of 1256 RWPs were found,
330 which corresponds to around 30 per season. Moreover, 141 were LLRWPs, that is about 11% of
331 the total RWPs. From the 141 LLRWPs, 45% have associated large-scale RWB, whereas for the
332 SLRWPs (1115 cases) this proportion is close to 39%. In both cases RWB events show
333 anticyclonic shear: 79% (76%) of the RWB episodes detected after the propagation of a LLRWP
334 (SLRWP) show anticyclonic RWB.

335 Figure 5 displays the frequency of occurrence of RWB events as a function of longitude that
336 happened after the end of a LLRWPs/SLRWPs. When we focus on the RWB events linked to the
337 end of LLRWPs propagation, (figure 5a), we observe that the distribution of these events is
338 displaced eastward. As Pérez *et al.*, (2021) showed, LLRWPs tend to last longer and propagate
339 further into the western Pacific due to an extension of the jet wave guide modulated by the SAM.

340 On the other hand, most of the wave breaking events that appear after the dissipation of
341 SLRWPs, (figure 5b), tend to occur between 120-180°E, which corresponds to the Indian-
342 western Pacific sector. This is similar to the results obtained in previous studies (Ndarana and
343 Waugh 2010 a,b). The results found here are consistent with these results, such that an extended
344 jet stream allows LLRWPs to propagate further east and break in the Pacific ocean, instead of in
345 the eastern Indian ocean sector. Thus, RWB events associated with LLRWPs tend to occur in the
346 middle-eastern Pacific basin, which could imply that long-lived packets might be precursors of
347 weather regime transitions affecting conditions in South America.

348 Figure 6 shows temporal and spatial characteristics of the RWB events detected after the
349 dissipation of LLRWPs and SLRWPs. In figure 6a we display the number of days that pass until
350 a RWB event is detected after the dissipation of a RWP. The two distributions are similar, that is,
351 most of the RWB events occur the same or the next day after the RWP dissipation, although we
352 observe more dispersion in the LLRWPs distribution. Additionally, figure 6b shows the lifespan
353 of the RWB events, indicating that most of the RWB events last between 1-2 days, and that there
354 are no significant differences between both distributions. Nonetheless, when we compare the
355 zonal extension of the wave breaking events, (figure 6c), RWB events that occur after the
356 propagation of SLRWPs cover larger longitudinal extensions compared to those observed after
357 LLRWPs. RWB events linked to LLRWPs show a median longitudinal extension of 22°, and a
358 interquartile range of 12°, whereas RWB associated to SLRWPs have a median of 26.5° and
359 display an interquartile range of 15°. A Kruskal-Wallis test applied to the datasets of figure 6c,
360 indicates that the distributions are significantly different, at 5% level of significance.

361 Hence, these results suggest that RWB events caused by SLRWPs cover larger longitudinal
362 extensions of the atmosphere compared to those produced by LLRWPs. Nonetheless, neither
363 LLRWPs or SLRWPs seem to be directly related to atmospheric blocking development because,
364 even if the associated RWB events have similar spatial scales to a blocking event, they tend to
365 last only about 1-2 days, too short to lead to blocking (see also section 5).

366 **4 Interannual variability of Rossby Wave Breaking events associated to LLRWPs/SLRWPs**

367 The interannual variability in the occurrence of RWB associated to LLRWPs and SLRWPs is
368 shown in figure 7. Both time series show large year-to-year variability. In the case of LLRWPs,
369 the number of annual RWB events range from 0 to 11, while for SLRWPs it ranges from 6 to 32.
370 During certain periods the frequency of occurrence of RWB associated to the LLRWPs and
371 SLRWPs seem to be out of phase, but no significant correlation has been found between the two
372 time series.

373 Figure 8 shows the temporal evolution of the RWB events linked to LLRWPs together with the
374 SAM/ENSO indices, this is, the Antarctic Oscillation Index for SAM and the Oceanic Niño
375 Index for ENSO. A correlation analysis indicates that there is no linear relationship between the
376 number of RWB events linked to the dissipation of LLRWPs with SAM or ENSO. It is also

377 worth noting that one reason that can influence the results is that we have several years without
378 RWB activity linked to LLRWPs, which can increase the difficulty of finding significant
379 correlation between the timeseries of RWB events linked to LLRWPs and SAM or ENSO
380 activity.

381 On the other hand, the interannual variability of RWB events linked to SLRWPs is correlated
382 with SAM/ENSO indices (Figure 9). Years with positive SAM have a higher frequency of
383 occurrence of RWB linked to SLRWPs, and the opposite occurs in years with negative SAM.
384 This is reflected in a Pearson correlation coefficient value of 0.25 between the Antarctic
385 Oscillation Index and the RWB events linked to SLRWPs, which is statistically significant at
386 10% level (using Student t-test). Moreover, a similar analysis indicates that the correlation
387 between the Oceanic Niño Index and RWB events linked to SLRWPs is -0.35, statistically
388 significant at 5% level. Thus, La Niña years tend to favor the development of RWB events,
389 whereas El Niño years do the opposite. In agreement, Wang and Magnusdottir (2010) and Gong
390 *et al.*, (2010) concluded that RWB in the tropical/subtropical Pacific is increased during La Niña
391 events, and this was associated to a strong local decrease in the zonal wind. At the same time
392 Barreiro (2017) found that El Niño events tend to favor the RWPs propagation. Therefore, El
393 Niño seems to induce large scale background conditions that favor the propagation of RWPs and,
394 by extension, diminishes the occurrence of RWB, whereas the wind flow decrease during La
395 Niña disfavors the propagation of RWPs and propitiates the occurrence of RWB events.

396 **5 Link between atmospheric blocking and large-scale Rossby Wave Breaking**

397 Results of section 3.2 suggest that the link between RWB associated with RWPs and blocking is
398 not obvious because these RWB events tend to last 1 or 2 days. Here we look further into the
399 relationship between RWB and blockings.

400 Table 1 shows the number of blocking events found as a function of the persistence and
401 longitudinal extension considered. For the less restrictive criteria (blocks that last at least 4 days
402 and with a minimum longitudinal extension of 7.5°) there are 263 events between 1979-2020
403 summertime, which corresponds to around 6 blocking events per season. This large number of
404 events reflects the fact that these criteria cause the finding of more blocking-like situations than
405 atmospheric blocks. On the other hand, for the most intense blocks (lifespan of 5 or more days
406 and with a minimum extension of 15°) there are 55 events, this is, a mean of 1.3 events per year.
407 As expected, we observe a decrease in blocking events as the conditions become more
408 restrictive.

409 It is worth mentioning that we find a mean of 3 atmospheric block events per year when we
410 follow the criteria of Mendes *et al.*, (2011), which is similar to the number they found (between
411 2.9-3.1 events per year).

412 In addition, when we focus on the detection areas of blockings, we find that near 50% of the
413 events appear at the central-western Pacific basin (181-240°E) independently of the zonal
414 extension and persistence of the event. On the other hand, there is a secondary area of blocking
415 development in the eastern Indian basin (121-180°E), where we find around 23-38% of the
416 blocking events, showing the highest (lowest) values during the strongest (weakest) blocking
417 events. Oppositely, we barely detect any blocking in the western south-Atlantic (300-359°E) or
418 the central Indian basin (0-60°E). These results are summarized in table 2 and are in accordance
419 with the observations in Hendes *et al.*, (2011).

420 The search for large-scale RWB associated to the formation of an atmospheric block reveals that
421 the latter appear close to a RWB event between 15-18% of the times independently of the
422 strength and stability of the block (not shown). Also, in agreement with the results of section 3.2,
423 we only found RWB linked to propagating RWPs near the development of an atmospheric block
424 around 3-6% of the times, and it does not seem to depend on the intensity and stability of the
425 block.

426 To summarize, RWB events are present in the atmosphere around 1 out of 5 times an
427 atmospheric block is detected in the atmosphere, but these RWB events do not seem to be related
428 with the propagating RWPs. Thus, propagating RWPs do not seem to be directly linked to the
429 development of atmospheric blocks. We recall that here we described propagating RWPs as those
430 with speed between 15-45°/day eastward, a zonal number between 4-12 days, and lifespan larger
431 than three days.

432 **6 Summary and conclusions**

433 Rossby Wave Breaking events are atmospheric perturbations that interfere in the wind and
434 energy flow, and under certain circumstances they can cause an atmospheric block, leading to the
435 development of heatwaves or droughts. In this work, an algorithm to track overturning regions of
436 potential vorticity was developed in order to identify Rossby Wave breaking areas that are linked
437 to the dissipation of transient Rossby Wave Packets.

438 We found that both long-lived Rossby Wave Packets and short-lived Rossby Wave packets tend
439 to show wave breaking events around 40% of the time, although this number is slightly higher
440 for long-lived packets. Rossby Wave breaking events that occur preceded by long-lived Rossby
441 Wave Packets tend to manifest at the center-eastern part of the Pacific basin, and are less zonally
442 extended compared to the wave breaking events associated with the rest of the packets.
443 Therefore, changes in weather regime conditions caused by wave breaking events that are linked
444 to long-lived Rossby Wave Packets are more likely to occur at the south of South America.
445 Moreover, wave breaking events linked to Rossby Wave Packets tend to last between 1-2 days in
446 the atmosphere for both long-lived and short-medium lived packets. Thus, wave breaking events
447 produced by propagating RWPs do not seem to be directly linked to the development of
448 atmospheric blocks.

449 Previous studies have found that negative SAM years are characterized by a larger number of
450 long-lived Rossby Wave Packets due to the extension of the Atlantic-Indian basin jet wave guide
451 into the Pacific (Pérez *et al.*, 2021). Here we report that the frequency of wave breaking linked to
452 long-lived Rossby Wave packets do not seem to be affected by SAM nor ENSO. On the
453 contrary, positive SAM conditions and La Niña events favor the development of wave breaking
454 episodes after the propagation of short-lived RWPs. Pérez *et al.*, (2021) concluded that the
455 frequency of occurrence of long-lived Rossby Wave packets is negatively correlated with the
456 number of short-lived Rossby Wave Packets. Thus, years with positive SAM conditions cause a
457 decrease in the number of long-lived Rossby Wave Packets and an increase of short-lived
458 packets. Consequently, the amount of Rossby Wave breaking events linked to Rossby Wave
459 Packets is expected to increase in years with positive SAM events. In addition, results also
460 suggest that RWB events are more common during years with La Niña.

461 Finally, we assess whether Rossby Wave Breaking events appear near the development of
462 atmospheric blocks, and found that around 1 out of 5 times a blocking event develops, a Rossby
463 Wave Breaking event is present. However, Rossby Wave Breaking linked to propagating Rossby
464 Wave Packets do not seem to be associated to atmosphere blocking development. Therefore,
465 blocking event development during southern hemisphere summertime might be linked to other
466 atmospheric perturbations not considered in this study such as stationary Rossby Wave packets,
467 propagating wave packets with very low wavenumber (1-3), or they might be triggered by other
468 atmospheric processes.

469 **Data availability Statement**

470 ERA5 reanalysis data are freely available in the Copernicus Climate Data Store
471 <https://cds.climate.copernicus.eu/>, whereas ENSO and SAM indexes are available at
472 <https://origin.cpc.ncep.noaa.gov/>. The wind envelope amplitude of the RWPs used in this study
473 is publicly available at <https://doi.org/10.5281/zenodo.5714192>, and a script describing how to
474 obtain wind envelope data from meridional wind speed at
475 <https://doi.org/10.5281/zenodo.5724656>.

476 **Acknowledgments**

477 This project has received funding from the European Union's Horizon 2020 research and
478 innovation programme under the Marie Skłodowska-Curie grant agreement No 813844 (ITN
479 CAFÉ). NE, CL and EHG acknowledge grant PID2021-123352OB-C32 funded by MCIN/AEI/
480 10.13039/501100011033 FEDER/UE.

481

482

483 **References**

- 484 Altenhoff, M, A., Martius, O., Croci-Maspoli, M.,Schwierz, C & Davies,C,H. (2008) Linkage of atmospheric blocking and
 485 synoptic-scale Rossby waves: a climatological analysis, *Tellus A: Dynamic Meteorology and Oceanography*, 60(5), 1053-1063,
 486 <https://doi.org/10.1111/j.1600-0870.2008.00354.x>
- 487 Barnes, A, E and Hartmann, L,D. (2012) Detection of Rossby wave breaking and its response to shifts of the midlatitude jet with
 488 climate change. *Journal of Geophysical Research*, 117(D9). <https://doi.org/10.1029/2012JD017469>
- 489 Berrisford, P., Hoskins, J, B and Tyrlis, E. (2007) Blocking and Rossby Wave Breaking on the Dynamical Tropopause in the
 490 Southern Hemisphere. *Journal of the Atmospheric Sciences*,64(8), 2881-2898. <https://doi.org/10.1175/JAS3984.1>
- 491 Chang, E. K. M. (1999) Characteristics of wave packets in the upper troposphere. Part II: Seasonal and hemispheric variations.
 492 *Journal of Atmospheric Sciences*, 56(11), 1729-1747. [https://doi.org/10.1175/1520-0469\(1999\)056<1729:COWPIT>2.0.CO;2](https://doi.org/10.1175/1520-0469(1999)056<1729:COWPIT>2.0.CO;2)
- 493 Chang, E. K. M., & D. B. Yu. (1999) Characteristics of wave packets in the upper troposphere. Part I:Northern Hemisphere
 494 winter. *Journal of Atmospheric Sciences*, 56(11), 1708-1728. [https://doi.org/10.1175/1520-0469\(1999\)056<1708:COWPIT>2.0.CO;2](https://doi.org/10.1175/1520-0469(1999)056<1708:COWPIT>2.0.CO;2)
- 495
- 496 Chang, E. K. M. (2000) Wave Packets and Life Cycles of Troughs in the Upper Troposphere: Examples from the Southern
 497 Hemisphere, Summer Season of 1984/1985. *Monthly Weather Reviewer*, 128(1), 25-50. [https://doi.org/10.1175/1520-0493\(2000\)128<0025:WPALCO>2.0.CO;2](https://doi.org/10.1175/1520-0493(2000)128<0025:WPALCO>2.0.CO;2)
- 498
- 499 Chang, E. K. M. (2005) The Impact of Wave Packets Propagating across Asia on Pacific Cyclone Development. *Monthly*
 500 *Weather Review*, Vol 133(7) 1998-2015. <https://doi.org/10.1175/MWR2953.1>
- 501 Gong, T., Feldstein, B. S., Luo, D. (2010) The Impact of ENSO on Wave Breaking and Southern Annular Mode Events.*Journal*
 502 *of the atmospheric Sciences*, 67(9), 2854-2870. <https://doi.org/10.1175/2010JAS3311.1>
- 503 Grazzini, F and Vitart F. (2015) Atmospheric predictability and Rossby wave packets. *International Journal. of the Royal .*
 504 *Meteorological. Society*, 141(692), 2793-2802. <https://doi.org/10.1002/qj.2564>
- 505 Hans, H., Bell, B., Berrisford, P., Hirahara, S., Horány, A.,Muñoz-Sabater, *et al.* (2020) The ERA5 global reanalysis. *Royal*
 506 *Meteorological Society*, 146(730), 1999-2049. <https://doi.org/10.1002/qj.3803>
- 507 Hitchman, H. M., and Huesmann,S,A. (2007) A seasonal clima-tology of Rossby wave breaking in the 320–2000-K layer.
 508 *J.Atmos. Sci.*, 64(6), 1922–1940. <https://doi.org/10.1175/JAS3927.1>
- 509 Holton, J. R., Haynes , H P., McIntyre, E. M., Douglass,R, A., Roodm. B., R and Pfister, L. (1995) Stratosphere–troposphere
 510 exchange. *Rev. Geophys.*, 33(4), 403–439. <https://doi.org/10.1029/95RG02097>
- 511 Hoskins,J,N., Ambrizzi, T. (1993) Rossby Wave Propoagation on a Realistic Longitudinally Varying Flow. *Journal of the*
 512 *Atmospheric Sciences*, 50(12). [https://doi.org/10.1175/1520-0469\(1993\)050<1661:RWPOAR>2.0.CO;2](https://doi.org/10.1175/1520-0469(1993)050<1661:RWPOAR>2.0.CO;2)

- 513 Hoskins J.B., McIntyre E.M., Robertson W.A. (1985) On the use and significance of isentropic potential vorticity maps. *Q. J. R.*
514 *Meteorol. Soc.* 111(470), 877–946. <https://doi.org/10.1002/qj.49711147002>
- 515 Masato, G., Hoskins, J.B., Woollings, T. (2011) Wave breaking characteristics of mid-latitude blocking. *Quarterly Journal of the*
516 *Royal Meteorological Society*, 138(666), 1285-1296. <https://doi.org/10.1002/qj.990>
- 517 Masato, G., Hoskins, J.B., Woollings, T. (2013) Wave-Breaking Characteristics of Northern Hemisphere Winter Blocking: A Two-
518 Dimensional Approach. *Journal of Climate*, 26(13), 4535-4549. <https://doi.org/10.1175/JCLI-D-12-00240.1>
- 519 Mendes, M. C. D., Cavalcanti, I. F., & Herdies, D. L. (2011) Southern Hemisphere atmospheric blocking diagnostic by ECMWF
520 and NCEP/NCAR data. *Revista Brasileira de Meteorologia*, 27(3), 263-271. <https://doi.org/10.1590/S0102-77862012000300001>
- 521 Michel, C and Rivière, G (2011) The Link between Rossby Wave Breaking and Weather Regime Transitions. *Journal of The*
522 *Atmospheric Sciences*, 68(8), 1730-1748. <https://doi.org/10.1175/2011JAS3635.1>
- 523 McIntyre, E. M., and Palmer, T.N (1983) Breaking planetary waves in the stratosphere. *Nature*, 305, 593–600.
524 <https://doi.org/10.1038/305593a0>
- 525 McIntyre, E. M and Palmer, T.N., Palmer, (1984) The “surf zone” in the stratosphere. *J. Atmos. Terr. Phys.*, 46(9), 825–839.
526 [https://doi.org/10.1016/0021-9169\(84\)90063-1](https://doi.org/10.1016/0021-9169(84)90063-1)
- 527 Ndarana, T and Waugh, D., (2010a) The link between cut-off lows and Rossby wave breaking in the Southern Hemisphere. *Q.J.R*
528 *Meteorol. Soc.* 136(649), 869-885. <https://doi.org/10.1002/qj.627>
- 529 Ndarana, T and Waugh, W,D (2010b) A climatology of Rossby Wave Breaking on the Southern Hemisphere Tropopause.
530 *Journal of the Atmospheric Sciences*, Vol 68, 798-811. <https://doi.org/10.1175/2010JAS3460.1>
- 531 O’Brien L., & Reeder, J. M. (2017) Southern Hemisphere Summertime Rossby Waves and Weather in the Australian Region.
532 *Quarterly Journal of the Royal Meteorological Society*. 143(707), 2374-2388. <https://doi.org/10.1002/qj.3090>
- 533 Patterson, M., Bracegirdle, T., & Woollings, T. (2019) Southern Hemisphere atmospheric blocking CMIP5 and future changes in
534 the Australia-New Zealand sector. *Geophysical Research Letters*, 46(15), 9281–9290. <https://doi.org/10.1029/2019GL083264>
- 535 Peters, D., and Waugh, W, D. (1996) Influence of barotropic shear on the poleward advection of upper-tropospheric air. *J. Atmos.*
536 *Sc.* 53(21), 3013–3031. [https://doi.org/10.1175/1520-0469\(1996\)053<3013:OBSOT>2.0.CO;2](https://doi.org/10.1175/1520-0469(1996)053<3013:OBSOT>2.0.CO;2)
- 537 Peters, D., and Waugh, W, D. (2003) Rossby wave breaking in the Southern Hemisphere wintertime upper troposphere. *Mon.*
538 *Wea. Rev.*, 131(11), 2623–2634. [https://doi.org/10.1175/1520-0493\(2003\)131<2623:RWBITS>2.0.CO;2](https://doi.org/10.1175/1520-0493(2003)131<2623:RWBITS>2.0.CO;2)
- 539 Pérez, I., Barreiro, M., & Masoller, C. (2021) ENSO and SAM influence on the generation of long episodes of Rossby Wave
540 Packets during Southern Hemisphere summer. *Journal of Geophysical Research: Atmospheres*, 126(24).e2021JD035467
541 <https://doi.org/10.1029/2021JD035467>
- 542 Rex, D. F. (1950) Blocking action in the middle troposphere and its effect upon regional climate. *Tellus*, 2(3), 196–211.
543 <https://doi.org/10.3402/tellusa.v2i4.8603>

- 544 Ryoo, J-M., Kaspi, Y., Waugh, W , D., Kiladis, N, G., Waliser, E, D., Fetzer, J, E and Jinwon, K. (2013) Impact of Rossby Wave
545 Breaking on U.S. West Coast Winter Precipitation during ENSO Events,*Journal of Climate*,26(17), 6360-6382.
546 <https://doi.org/10.1175/JCLI-D-12-00297.1>
- 547 Sagarra, R., & Barreiro, M. (2020) Characterization of extratropical waves during summer of the Southern Hemisphere.
548 *Meteorologica*, 45(2), 63-79. <https://hdl.handle.net/20.500.12008/33550>
- 549 Simmons, J. A., and Hoskins,J,B (1978) The life cycles of somenonlinear baroclinic waves. *J. Atmos. Sci.*, 35(3), 414–432.
550 [https://doi.org/10.1175/1520-0469\(1978\)035<0414:TLCOSN>2.0.CO;2](https://doi.org/10.1175/1520-0469(1978)035<0414:TLCOSN>2.0.CO;2)
- 551 Souders, B. M., Colle, A. B., & Chang, M. K. E. (2014a) The climatology and characteristics of Rossby Wave Packets using a
552 feature-based tracking technique. *Monthly Weather Review*, 142(10), 3528–3548. <https://doi.org/10.1175/MWR-D-13-00371.1>
- 553 Souders, B. M., Colle, A. B., & Chang, M. K. E. (2014b) A Description and Evaluation of an Automated Approach for Feature-
554 Based Tracking of Rossby Wave Packets. *Monthly Weather Review*, 142(10), 3505–3527. <https://doi.org/10.1175/MWR-D-13-00317.1>
555
- 556 Strong, C and Magnusdottir, G. (2008) Tropospheric Rossby Wave Breaking and the NAO/NAM, *Journal of the Atmospheric*
557 *Sciences*,65(9), 2861-2876 <https://doi.org/10.1175/2008JAS2632.1>
- 558 Tibaldi, S. and Molteni, F (1990) On the operational predictability of blocking. *Tellus A*, 42, 343-365.
559 <https://doi.org/10.1034/j.1600-0870.1990.t01-2-00003.x>
- 560 Thorncroft, D. C., Hoskins, J, B, and McIntyre,E,M (1993) Two paradigms of baroclinic-wave life-cycle behaviour. *Quart. J.*
561 *Roy. Meteor. Soc.*, 119(509), 17–55.<https://doi.org/10.1002/qj.49711950903>
- 562 Trenberth, E. K. (1981). Observed Southern Hemisphere Eddy Statistics at 500 mb: Frequency and Spatial Dependence. *Journal*
563 *of Atmospheric Science*, 38(12), 2585–2605. [https://doi.org/10.1175/1520-0469\(1981\)038<2585:OSHESA>2.0.CO;2](https://doi.org/10.1175/1520-0469(1981)038<2585:OSHESA>2.0.CO;2)
- 564 Wang, Y and Magnusdottir, G (2010) Tropospheric Rossby Wave Breaking and the SAM, 24(8), 2134-2146,
565 <https://doi.org/10.1175/2010JCLI4009.1>
- 566 Wiedenmann, M,J., Lupo,R,A., Mokhov, I, I and Tikhonova, A, E. (2002) *Journal of Climate*, 15(23), 3459-3473.
567 [https://doi.org/10.1175/1520-0442\(2002\)015<3459:TCOBAF>2.0.CO;2](https://doi.org/10.1175/1520-0442(2002)015<3459:TCOBAF>2.0.CO;2)
- 568 Wirth, V., Riemer, M., Chang, E, K, M., & Martius, O. (2018) Rossby Wave Packets on the Midlatitude waveguide- a review.
569 *Monthly Weather Review*, 146(7), 1965-2001. <https://doi.org/10.1175/MWR-D-16-0483.1>
- 570 Wirth, V. (2020) Waveguidability of idealized midlatitude jets and the limitations of ray tracing theory. *Weather Climate*
571 *Dynamics*, 1, 111–125. <https://doi.org/10.5194/wcd-1-111-202>
- 572 Woollings, T., Barriopedro, D., Methven, J., Son, S.-W., Martius, O., Harvey, B., et al. (2018) Blocking and its response to
573 climate change. *Current Climate Change Reports*, 4, 287–300. <https://doi.org/10.1007/s40641-018-0108-z>

574 Yeh, T. C. (1949) On energy dispersion in the atmosphere. *Journal of Meteorology*, 6(1), 1–16. [https://doi.org/10.1175/1520-0469\(1949\)006<0001:OEDITA>2.0.CO;2](https://doi.org/10.1175/1520-0469(1949)006<0001:OEDITA>2.0.CO;2)

576 Zheng, M., Chang, E. K., & Colle, B. A. (2013) Ensemble sensitivity tools for assessing extratropical cyclone intensity and track predictability. *Weather and forecasting*, 28(5), 1133-1156.. <https://doi.org/10.1175/WAF-D-12-00132.1>

578 **Tables**

	7.5° L	10°L	12.5°L	15°L
4d	263	212	168	123
	7.5°L	10°L	12.5°L	15°L
5d	142	107	79	55

579 **Table 1.** Number of blocking events found using different criteria, (d) refers to minimum
 580 lifespan in days and (L) the minimum longitudinal extension in degrees of the atmospheric
 581 blocks detected.

582

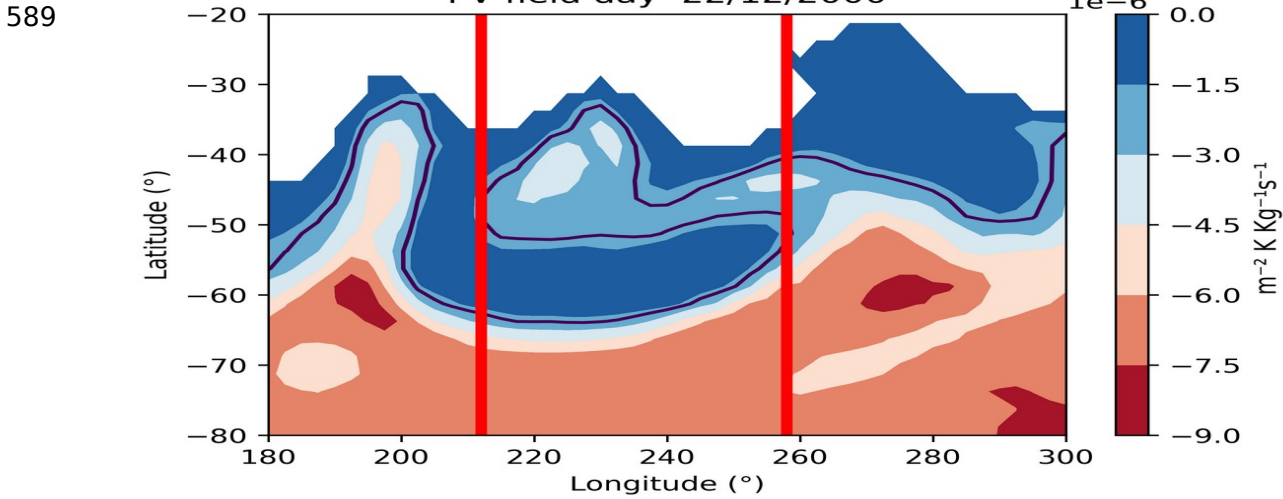
	Eastern South-Atlantic- western Indian basin (0- 60°E)	Central Indian basin (61-120°E)	Eastern Indian basin (121-180°E)	Western Pacific basin (181-240°E)	Eastern Pacific basin (241-300°E)	Western South- Atlantic (301-359°E)
4d 7.5° L	10	16	63	118	38	18
5d 15° L	1	2	20	27	4	1

583 **Table 2.** Number of summertime blocking events between 1979 and 2020 in the area of study for
 584 two blocking detection criteria: (d) refers to minimum lifespan of the event in days, and (L) to its
 585 minimum longitudinal extension in degrees.

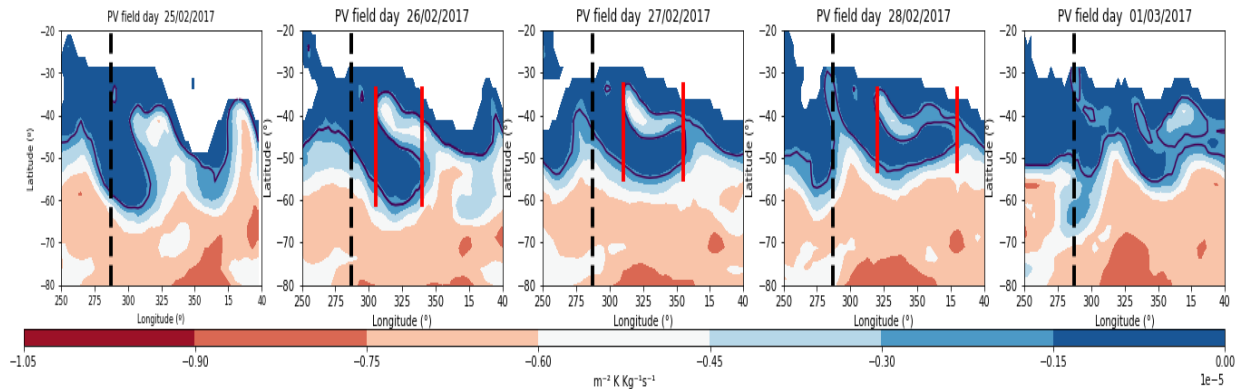
586

587

588 **Figures**

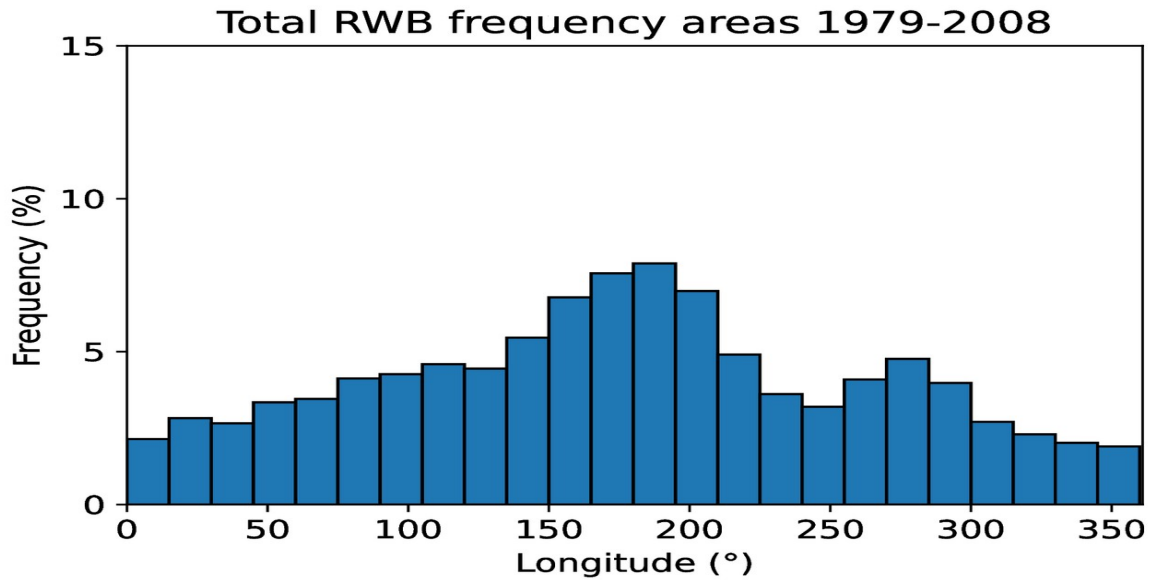


590 **Figure 1.** Potential vorticity fields following the 330°K isentropic isosurface during an anticyclonic RWB
 591 event detected on 22/12/2000. Red lines indicate the longitudinal section where the algorithm found the
 592 RWB event and the black line signals the location of the -2PVU line.

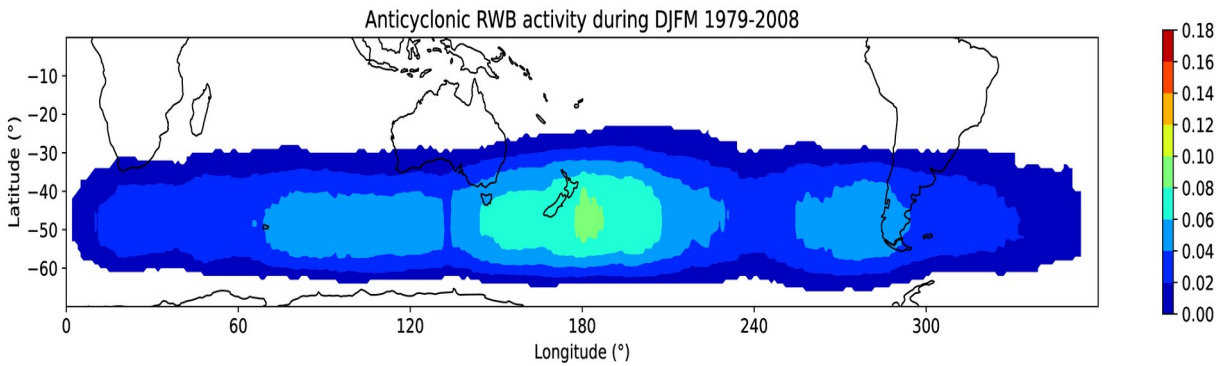


593 **Figure 2.** Potential vorticity fields following the 330°K isosurface between 25/02/2017-01/03/2017. The
 594 dashed black line shows the longitudinal section where a LLRWPs stopped its propagation at 25/02/2017,
 595 red lines indicate the area of RWB detected by the wave breaking algorithm and the black line signals the
 596 location of the -2PVU line.

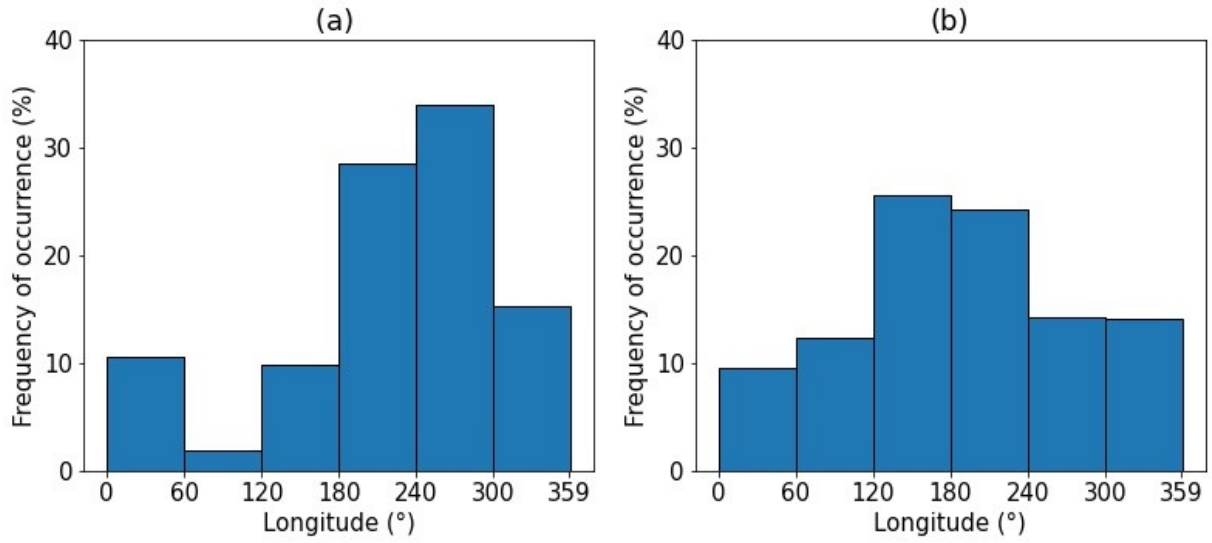
597



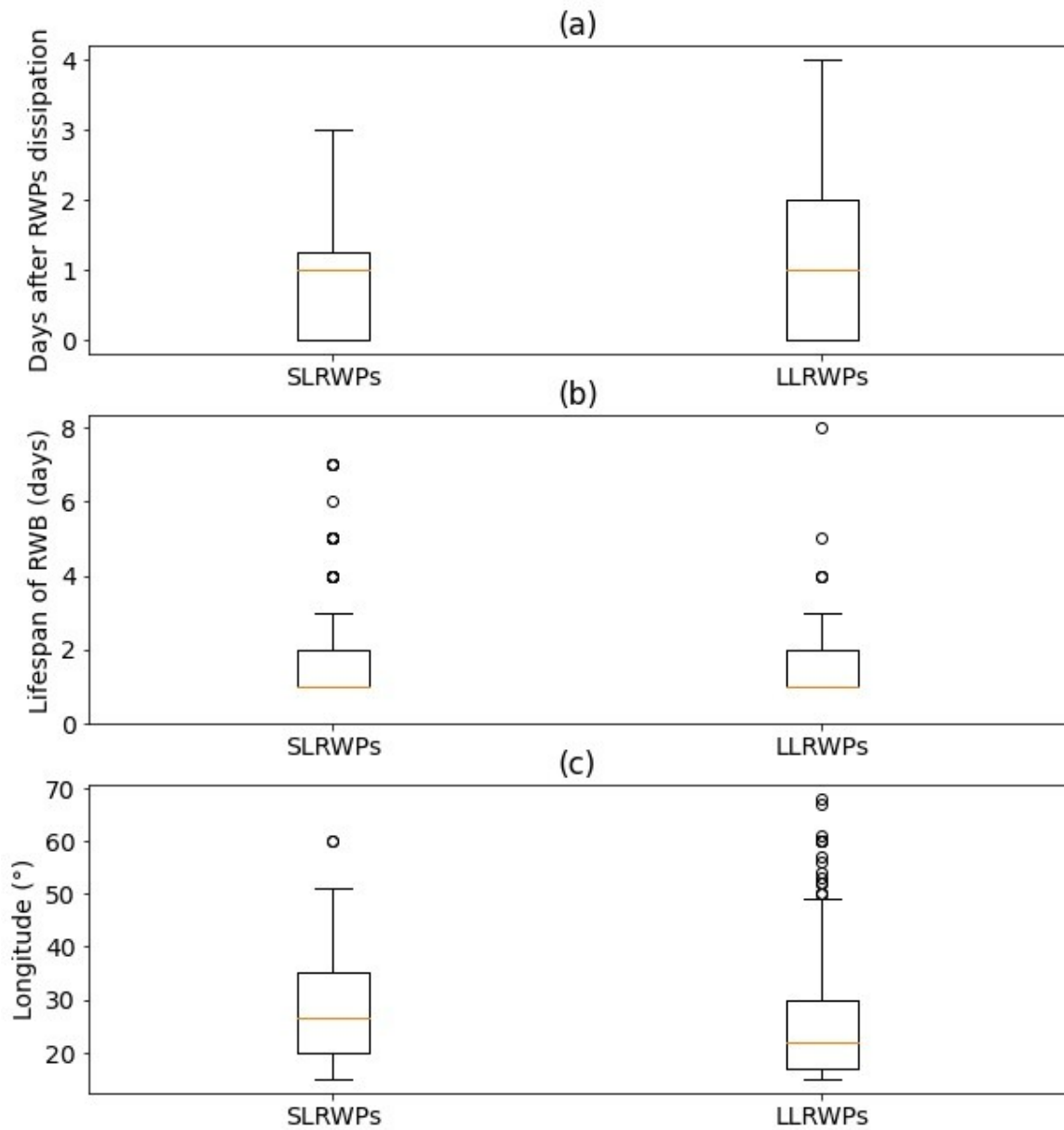
598 **Figure 3.** Frequency of RWB events found during summertime in the Southern Hemisphere between
599 1979-2008.



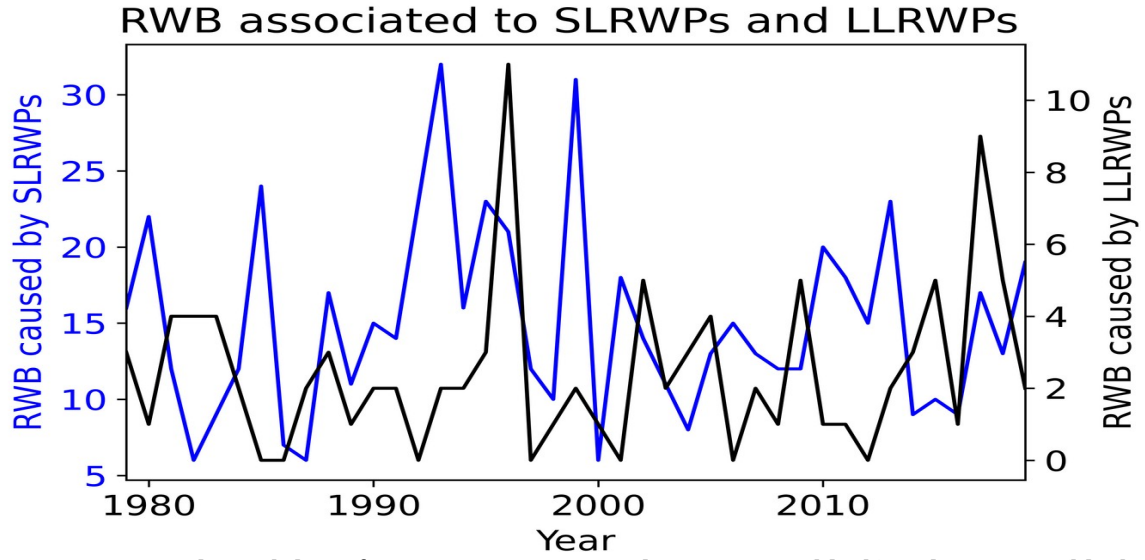
600 **Figure 4.** Anticyclonic RWB frequency found between 1979-2008. Colored areas show where RWB
601 episodes where detected.



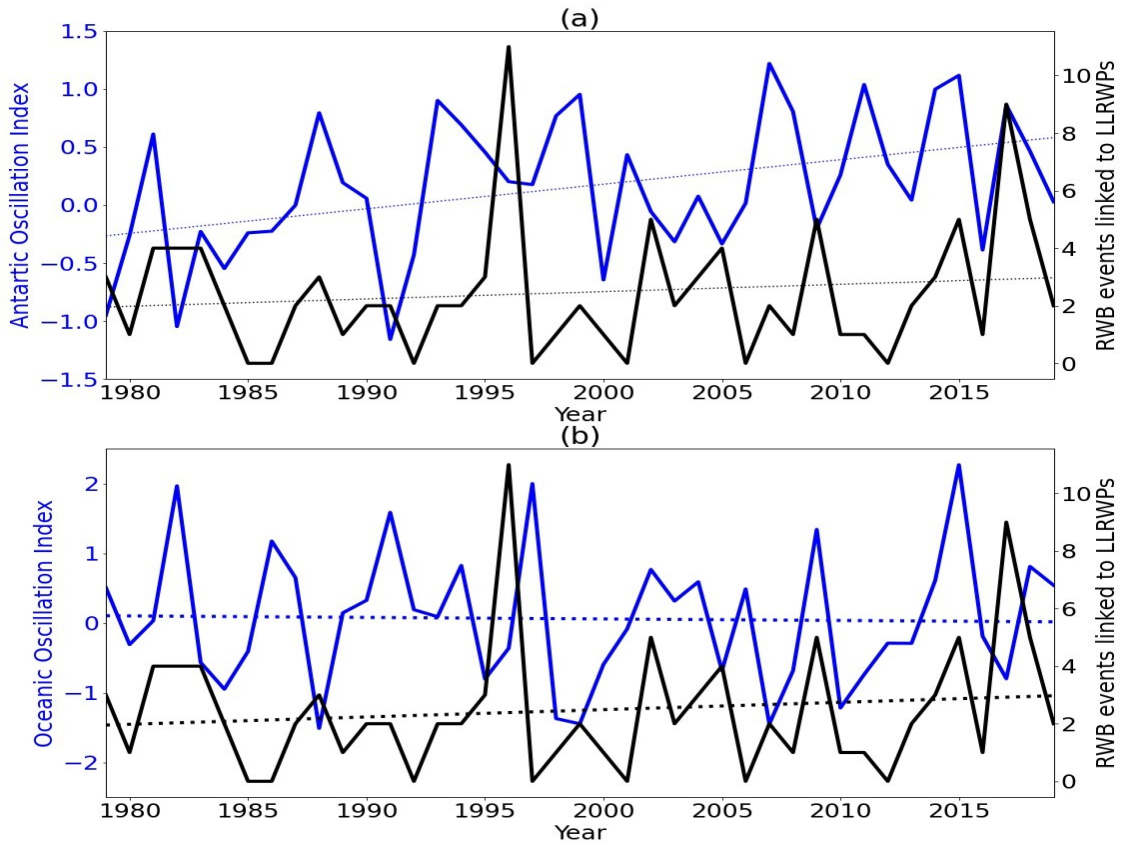
602 **Figure 5.** Relative frequency of occurrence of large-scale RWB associated to (a) LLRWPs and (b)
603 SLRWPs.



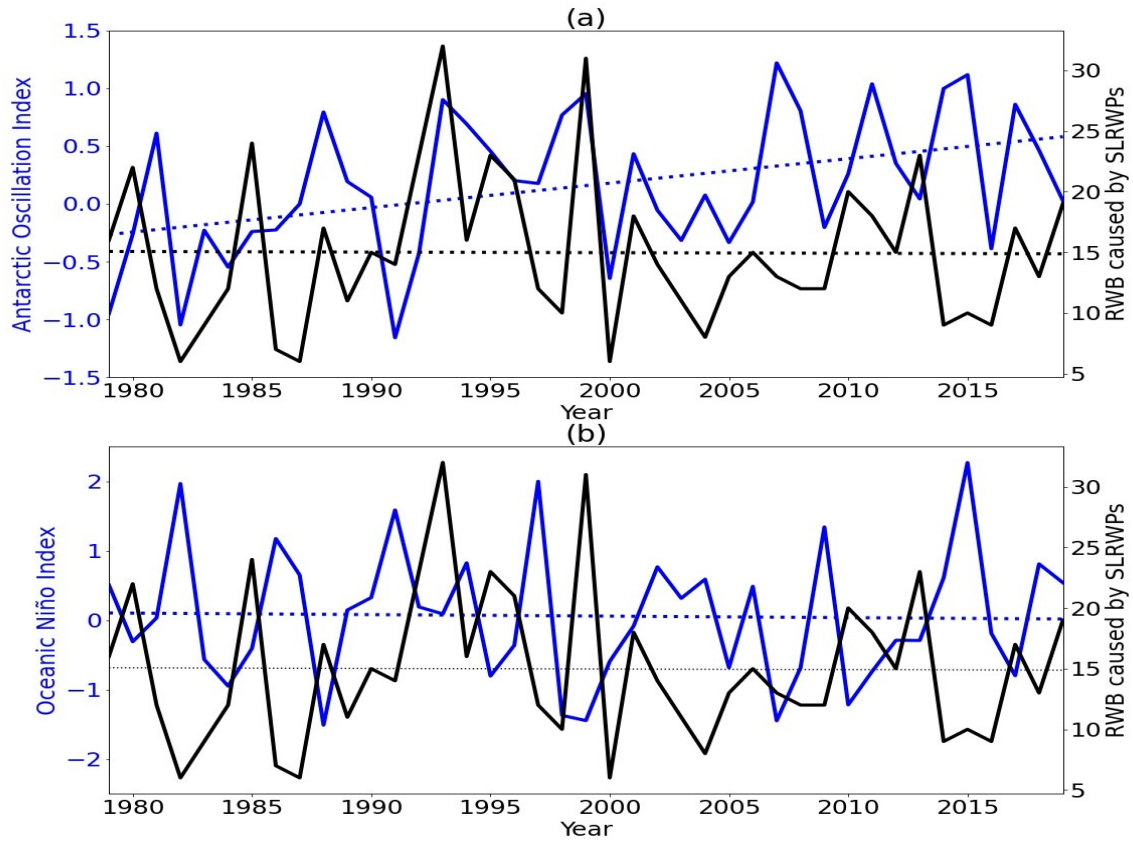
604 **Figure 6.** Boxplot distribution of several characteristics of RWB associated with LLRWPs and SLRWPs.
 605 Yellow lines in the boxplots signal the location of the median of the distribution. Upper figure (a) shows
 606 the day when a large-scale RWB event appears after the end of the RWPs propagation, middle figure (b)
 607 displays the mean lifespan of the RWB events, whereas the last figure shows the longitudinal extension of
 608 the RWB.



609 **Figure 7.** Interannual variability of RWB events associated to LLRWPs (black) and SLRWPs (black
610 lines).



612 **Figure 8.** Timeseries of annual RWB events associated to LLRWPs (black lines), against the temporal
 613 evolution of Oceanic Niño Index (a) and Antarctic Oscillation Index (b) during the period of study (blue
 614 lines). Dotted lines show the trend for each timeseries.



615 **Figure 9.** Timeseries of annual RWB events associated to SLRWPs (black lines), against the temporal
 616 evolution of Oceanic Niño Index (a) and Antarctic Oscillation Index (b) during the period of study (blue
 617 lines). Dotted lines show the trend for each timeseries.

1
2 **Wave Breaking Events and their link to Rossby Wave Packets and Atmospheric**
3 **Blockings during Southern Hemisphere Summer**
4

5 Iago Pérez-Fernández¹ , Marcelo Barreiro¹ , Noémie Ehstand² , Emilio Hernández-García² ,
6 Cristobal López² .

7 ¹*Departamento de Ciencias de la atmósfera y Física de los Océanos, Facultad de Ciencias, Universidad de la*
8 *República, Montevideo, Uruguay.*

9 ²*Instituto de Física Interdisciplinar y Sistemas Complejos (IFISC), CSIC-UIB. Palma de Mallorca, Spain.*

10 Corresponding author: Iago Pérez-Fernández (iperez@fisica.edu.uy)

11 **Key Points:**

- 12 • Large-scale wave breaking events caused by propagating Rossby Wave Packets do not
13 usually last enough to develop into an atmospheric block.
- 14 • Years with La Niña and positive Southern Annular Mode favor large-scale wave breaking
15 activity linked to short-lived Rossby Wave packets.
- 16 • Near 17% of blocking events appear preceded by a wave breaking event but most of them
17 are not linked to propagating Rossby Wave Packets.

18 **Abstract**

19 Rossby Wave packets (RWPs) are atmospheric perturbations located at upper levels in mid-latitudes which, in certain cases,
20 terminate in Rossby Wave Breaking (RWB) events. When sufficiently persistent and spatially extended, these RWB events are
21 synoptically identical to atmospheric blockings, which are linked to heatwaves and droughts. Thus, studying RWB events after
22 RWPs propagation and their link with blocking is key to enhance extreme weather events detection 10-30 days in advance.
23 Hence, here we assess (i) the occurrence of RWB events after the propagation of RWPs, (ii) whether long-lived RWPs (RWPs
24 with a lifespan above 8 days, or LLRWPs) are linked to large-scale RWB events that could form a blocking event, and (iii) the
25 proportion of blocking situations that occur near RWB events. To do so, we applied a tracking algorithm to detect RWPs in the
26 Southern Hemisphere during summertime between 1979-2020, developed a wave breaking algorithm to identify RWB events,
27 and searched for blocking events with different intensities. Results show that LLRWPs and the other RWPs displayed large-scale
28 RWB events around 40% of the time, and most RWB events in both distributions last around 1-2 days, which is not long enough
29 to identify them as blocking situations. Nearly 17% of blockings have a RWB event nearby, but barely 5% of blockings are
30 linked to RWPs, suggesting that propagating RWPs are not strongly linked to blocking development. Lastly, large-scale RWB
31 events associated with RWPs that lasted less than 8 days are influenced by the Southern Annular Mode and El Niño-Southern
32 Oscillation.

33 **Plain Language Summary**

34 When an atmospheric wave breaks in the upper level of the atmosphere, it modifies the wind flow and local weather conditions.
35 If these wave breaking events are sufficiently big and stable, they can produce atmospheric blocking events, which are linked to
36 heatwaves and drought development. In this study, we assess if a link between wave breaking events caused by long-lived
37 traveling atmospheric waves (atmospheric waves that last more than 8 days in the atmosphere) and blocking events development
38 exists during Southern hemisphere summer. Independently of the duration of the wave packets, near 4 out of 10 times they cause
39 very extensive wave breaking events, but they do not last long enough to be considered an atmospheric blocking. Oppositely,
40 nearly 20% of blocking events manifest nearby a wave breaking event independently of the strength of the block, but these wave
41 breaking events do not seem to be linked to traveling wave packets. Therefore, this study suggests that traveling atmospheric
42 waves are not directly related to the development of atmospheric blockings. Also, the occurrence of extensive wave breaking
43 events caused by traveling atmospheric waves that last less than 8 days are affected by phenomena like El Niño or the Southern
44 Annular Mode.

45 **Keywords** — Rossby Wave Packets, Wave Breaking, ENSO, SAM, Atmospheric Blocking

46 **1 Introduction**

47 Rossby Wave Packets (RWPs) are synoptic scale perturbations that appear in the upper
48 atmosphere of mid-latitudes. During their propagation, these packets travel by downstream
49 development mechanisms, transporting large quantities of energy in the process (Tu-Cheng Yeh
50 1949, Chang and Yu 1999; Chang 2000). RWPs play an important role in the global atmospheric
51 circulation because they are related to storm track variability (Souders *et al.*, 2014a). In addition,
52 they are precursors of extreme weather events such as heatwaves, extreme rainfall (Chang 2005;
53 Grazzini and Vitart 2015, O'Brien and Reeder 2017, Wirth *et al.*, 2018) and extratropical cyclone
54 development (Chang *et al.*, 2005, Sagarra and Barreiro 2020). Also, during their propagation
55 they increase the uncertainty of middle-long range forecast (from 3 to >10 days in advance) in
56 the areas they cross (Zheng *et al.*, 2013). Normally, these packets tend to last between 3-6 days
57 in the atmosphere but, under certain circumstances, they can last up to 2-3 weeks before
58 disappearing (e.g. Pérez *et al.*, 2021). When RWPs have a lifespan longer than 8 days, they are
59 referred to as long-lived RWPs or LLRWPs (Grazzini and Vitart 2015).

60 The lifespan and propagation of the RWPs greatly depend on the potential vorticity gradients and
61 the locations of diabatic heating sources (Grazzini and Vitart 2015). Potential vorticity gradients
62 shape the waveguide where the RWPs propagate, such that a very zonal and intense jet with

63 narrow potential vorticity gradients favor the development of very stable RWPs (Chang & Yu
64 1999, Souders *et al.*, 2014b, Wirth *et al.*, 2020), whereas weaker gradients damp or stop the
65 wave packets propagation (Grazzini and Vitart 2015).

66 Due to the lack of large baroclinically unfavorable areas in the Southern Hemisphere, RWPs are
67 easier to detect than in the Northern Hemisphere (Grazzini and Vitart 2015). In addition, during
68 austral summer (December to March) the jet stream displays a very zonal and narrow wind flow,
69 which acts as a waveguide where RWPs propagate (Hoskins & Ambrizzi, 1993; Chang, 1999),
70 and facilitates RWPs detection. Pérez *et al.*, (2021) showed that the Southern Annular Mode
71 (SAM) heavily influences the development of LLRWPs during austral summer, such that years
72 with positive SAM disfavor LLRWPs development whereas negative SAM favor them.
73 Conversely, El Niño-Southern Oscillation (ENSO) influence was found to be less robust.

74 When RWPs reach the end of their life cycle they can “break”, causing an irreversible mixing of
75 potential vorticity fields over a longitudinally confined region (Simmons and Hoskins 1978,
76 McIntyre and Palmer 1983, 1984). As a result, high potential vorticity air intrudes the
77 troposphere and/or low potential vorticity air enters in the stratosphere, causing the development
78 of potential vorticity anomalies that can either remove or reverse the usual potential vorticity
79 meridional gradients. This process is called Rossby Wave Breaking or RWB (McIntyre and
80 Palmer 1983, 1984, Berrisford *et al.*, 2007, Masato *et al.*, 2011). RWB events are key to the air
81 mass exchange between the troposphere and the stratosphere (Holton *et al.*, 1995), and are
82 considered as potential precursors of weather regime transitions (Michel and Rivière 2011) that
83 can increase the prediction skill of precipitation (Ryo *et al.*, 2013). In addition, RWB events
84 share some characteristics with atmospheric blocking. In fact, RWB events that show a spatial
85 and temporal scale similar to atmospheric blocking are synoptically recognized as a blocking
86 (Berrisford *et al.*, 2007). An atmospheric blocking event is a nearly-stationary large-scale pattern
87 in the pressure field arising from the reversal of the westerly wind flow, and it is stable enough to
88 last from several days to weeks in the atmosphere (Rex, 1950, Patterson *et al.*, 2019). Its
89 appearance is linked to the development of extreme weather events such as heatwaves or
90 droughts (Woollings, *et al.*, 2018). Nonetheless, even if we find some RWB events prior to the
91 onset of some atmospheric blockings (Altenhoff *et al.*, 2008), not all events are associated with
92 blocking (Hitchman and Huesmann 2007, Masato *et al.*, 2013).

93 There are two main types of RWB (Thorncroft *et al.*, 1993), one is cyclonic RWB, where low
94 potential temperature or “cold” air from the dynamical tropopause moves eastward and
95 equatorward to the west of high potential temperature air or “warm” air, whereas “warm” air
96 goes poleward and westward. The other is anticyclonic RWB, where the equatorward and
97 westward movement of low potential temperature air is to the east of the poleward and eastward
98 movement of the “warm” air. Each morphology of wave breaking implies different changes in
99 synoptic circulation. Anticyclonic RWB occurs with much more frequency than cyclonic RWB

100 because RWPs propagating in the tropopause tend to break in an anticyclonic fashion
101 (Thorncroft *et al.*, 1993; Peters and Waugh 1996, 2003).

102 Several studies of RWB were done for the Northern Hemisphere (e.g. Strong and Magnusdottir
103 2008, Masato *et al.*, 2011, Michel and Rivi re 2011, Ryoo *et al.*, 2013). For example, Thorncroft
104 *et al.* (1993) found that RWB frequency is influenced by processes that alter the wind flow. In
105 that regard, Strong and Magnusdottir (2008) concluded that the positive phase of the Northern
106 Annular Mode is associated with anticyclonic RWB, whereas its negative phase is linked to
107 cyclonic RWB. In the Southern Hemisphere, Berrisford *et al.*, (2007) showed that RWB in mid
108 latitudes wintertime is concentrated in the east Pacific, whereas during summertime RWB
109 episodes are less frequent and are confined to the west Pacific. This is in (qualitative) agreement
110 with the observed location of Southern hemisphere blocking. Gong *et al.*, (2010) studied the
111 influence of SAM and ENSO on RWB breaking during austral spring-summer, and found that
112 the positive phase of SAM shows higher wave breaking activity than the negative. Additionally,
113 Wang and Magnusdottir (2010) observed that anticyclonic and cyclonic RWB frequency is
114 affected by the changes in background flow caused by ENSO events.

115 A question still unanswered is the relationship between the occurrence of RWB and the
116 propagation of RWPs in the Southern hemisphere, as well as whether RWPs can cause RWB
117 events that can trigger atmospheric blocking development. Thus, the aim of this research is to
118 study the detection and evolution of RWB events after the propagation of transient RWPs, with
119 special emphasis on large-scale RWB. In addition, we classified the RWB considering whether
120 their associated RWPs is a LLRWPs or not. This is done in order to assess whether the wave
121 breaking events caused by LLRWPs share different characteristics as the those found for the rest
122 of the RWPs, and study whether RWB events that occur after the dissipation of a LLRWPs are
123 linked to the development of atmospheric blocking.

124 The paper is organized as follows. Section 2 describes the datasets and the methodologies for
125 tracking RWPs, detecting RWB events, as well as blockings. Section 3 focuses on the link
126 between RWB and RWPs, section 4 on the interannual variability of RWB events and the
127 potential impact of global climate modes, and section 5 assesses the link between atmospheric
128 blocking and RWB events. Finally, section 6 presents a summary of the study.

129 **2 Data and methodology**

130 2.1 Data

131 In this study, we used ERA 5 Reanalysis (Hans *et al.*, 2020), with an horizontal resolution of
132 $0.25^\circ \times 0.25^\circ$ and daily frequency. The region of study consists of the mid-latitudes of the
133 Southern Hemisphere, during austral summer (December to March or December-March)
134 between 1979-2021 as done in previous studies (Sagarra and Barreiro 2020, P rez *et al.*, 2021).
135 Thus, we have 41 seasons available for the analysis.

136 RWPs propagate in the upper atmosphere of mid-latitudes and manifest as meanders of the jet
137 stream. During their propagation, they produce a series of troughs and ridges that travel confined
138 to a certain latitudinal band, moving mainly eastward during austral summer (Chang 1999).
139 Thus, by computing the envelope of the meridional wind speed at 300 hPa ($V_{300\text{env}}$), we can
140 characterize these transient RWPs. To calculate the $V_{300\text{env}}$, we followed the methodology
141 specified in Pérez *et al.*, (2021). Next, due to the fact that RWPs propagation is mostly zonal
142 during December-March season (Chang 1999), we averaged the $V_{300\text{env}}$ data between the
143 latitudinal range of 40-65°S.

144 Regarding the detection of RWB events, as in previous studies, we have used the potential
145 vorticity field in isentropic coordinates, searching for areas where the usual meridional potential
146 vorticity gradient either disappears or is inverted. The computation of the potential vorticity field
147 was performed following Hoskins *et al.*, (1985), using daily temperature and wind speed at 300
148 hPa interpolated to the isentropic coordinates of 330°K.

149 Also, to characterize the interannual variability and amplitude of the global climate modes, we
150 used the Oceanic Niño Index for ENSO, and the Antarctic Oscillation index for SAM. Both
151 datasets are publicly available in the NOAA website (<https://origin.cpc.ncep.noaa.gov/>).

152 2.2 Description of Rossby Wave Packet tracking algorithm

153 The RWPs are detected using a tracking algorithm, based on the maximum envelope technique
154 (Grazzini and Vitart 2015, Sagarra and Barreiro 2020, Pérez *et al.*, 2021). This algorithm
155 searches for areas with the highest daily values of $V_{300\text{env}}$, identifying the center of activity of the
156 RWPs, and then follow the propagation of the wave packets to the east, assuming that they travel
157 between 15-45°E per day. Before applying the tracking algorithm, we filter out small values of
158 $V_{300\text{env}}$ to avoid tracking noise. Although there is no optimum threshold because there are no
159 physical properties that separate one wave packet from another (Souders *et al.*, 2014b), here we
160 applied a minimum threshold of 19 m/s. Pérez *et al.*, (2021) show that the tracking of RWPs is
161 not sensitive to the choice of threshold between 17-21 m/s.

162 It is also worth pointing out that the tracking algorithm only follows transient RWPs that is,
163 RWPs that propagate eastwards and have a zonal wavenumber between 4-11, which corresponds
164 to the transient structures of the Southern Hemisphere (Trenberth 1981). Therefore, the algorithm
165 cannot track stationary RWPs, or those RWPs with a wavenumber ≤ 3 . Hereafter, when we talk
166 about RWPs, we are referring to these transient RWPs.

167 After the algorithm finishes tracking all the RWPs of the season, it uses proximity criteria to link
168 trajectories of the RWPs that were interrupted, and then measures the characteristics of the
169 tracked wave packet: longitudinal extension, areas of formation/dissipation, lifespan and
170 propagation speed. The full description of the algorithm is available in Pérez *et al.*, (2021).

171 Finally, for the subsequent analysis, the tracked RWPs are classified in LLRWPs (lifetime >8
172 days) and short lived RWPs or SLRWPs (lifetime ≤ 8 days).

173 2.3 Rossby Wave Breaking detection algorithm and validation

174 As we mentioned in section 2.1, RWB events manifest in the upper atmosphere in areas where
175 the usual meridional gradient of potential vorticity either disappears or reverses. We can detect
176 these areas by locating where the potential vorticity contour lines overturn following isentropic
177 coordinates (McIntyre and Palmer 1983). Previous studies in the Southern Hemisphere followed
178 potential vorticity contours in the isolines between 310-350°K (Ndarana and Waugh 2010 a, b,
179 Strong and Magnusdottir 2008) because they represent the dynamical tropopause between the
180 high latitudes and the subtropics (Ndarana and Waugh 2010 a).

181 We choose to study RWB events that occur in the potential vorticity of -2 PVU ($1 \text{ PVU} = 10^{-6}$
182 $\text{m}^2 \text{ s}^{-1} \text{ K kg}^{-1}$) on the 330°K isosurface. The reason to chose this specific isosurface is because it
183 is a transitional region between the isosurface 310-350°K, where anticyclonic and cyclonic shear
184 have been found (Ndarana and Waugh 2010 a, b).

185 In order to identify RWB events we developed an objective algorithm based on the methodology
186 of Barnes and Hartmann (2012). The steps of the algorithm are the following:

187 1.- Representation of the -2 PVU contour line for day t , and retention of the longest contour line.
188 This is done to avoid the detection of isolated potential vorticity “bubbles” as part of RWB
189 events.

190 2.- Identification of areas where -2 PVU contours crosses more than 2 times the same
191 longitudinal section. These points are referred as wave breaking points.

192 3.- If there are wave breaking points closer than 500 km from each other we assumed that these
193 points belong to the same wave breaking event (Barnes and Hartmann 2012).

194 4.- Retention of RWB events that have a longitudinal extension $\geq 5^\circ$. This avoids registering
195 meridionally extended potential vorticity tongues that do not show overturning.

196 5.- Classification of the RWB event regarding their orientation. This is done by measuring the
197 latitudinal mean of the 4 most eastward and westward overturning points of the RWB episode. In
198 the Southern Hemisphere, cyclonic RWB events have their western-most overturning point
199 located equatorward, while their east-most overturning point is poleward. By contrast, in
200 anticyclonic RWB events their eastern-most overturning point are equatorward whereas their
201 west-most overturning point are poleward. Thus, if the latitudinal mean of their most westward
202 points of the contour is closer to poleward latitudes than the observed at the most eastward
203 points, we assume that the wave packet shows an anticyclonic shear, whereas if the most
204 westward points are closer to the equator than the most eastward points, the breaking event is

205 classified as cyclonic RWB. An example of the application of the RWB tracking algorithm can
206 be seen in figure 1.

207 6.- Measurement of the RWB characteristics: longitudinal and latitudinal extension of the event,
208 day of detection, and type of RWB shear.

209 7.- Repeat steps 1-6 for the following days until all the data is analyzed.

210 Given the few studies reported on RWB for the Southern hemisphere it is important first to
211 ensure that the detection algorithm works as expected. To do so, we first tracked wave breaking
212 events in the December-March season only between 1979-2008, and compared our results
213 against previous studies (Ndarana and Waugh 2010 a,b, Wang and Magnusdottir 2010).

214 2.4 Linking large-scale Rossby wave breaking events to Rossby Wave Packets

215 In this section we explain the methodology used to link RWB activity to the dissipation of
216 RWPs. At the moment of writing this article, the authors were not able to find a study which
217 links RWB events with RWPs in the Southern Hemisphere.

218 Before describing the methodology, it is important to highlight that in this section we will only
219 consider large-scale RWB, that is RWB events with a longitudinal extension of 1000 km ($\sim 15^\circ$ in
220 mid latitudes) or above (Barnes and Hartmann 2012). This is done in order to retain wave
221 breaking events that can strongly affect the large-scale atmospheric circulation and have a spatial
222 scale similar to atmosphere blocking, (11° of extension, Patterson *et al.*, 2019).

223 The methodology used for linking RWPs with RWB events has the following steps:

224 1.-Apply the RWB tracking algorithm at day T_f , being T_f the day when a RWP finished its
225 propagation.

226 2.-If the algorithm detects the beginning of a RWB event located between $X_f \pm 2000$ km, being
227 X_f the longitudinal section where the algorithm located a RWPs before stopping its propagation,
228 we assume that the wave breaking event registered is linked to the RWP that stopped its
229 propagation and we proceed to step 3. If the described condition is not fulfilled, we continue
230 looking for RWB events for the following days. If by day T_{f+4} we do not find a RWB event that
231 matches the described condition, we assumed that the RWP did not show a RWB episode and
232 finish the search. Oppositely, if after applying the wave breaking detection algorithm we detect
233 two or more RWB event which are in the range $X_f \pm 2000$ km, we select the RWB whose
234 geographical center is closer to the area of dissipation of the RWP.

235 3.-We register the day when a RWB event is detected as T_n , and applied the RWB tracking
236 algorithm at day T_{n+1} . If a RWB event exists with geographical center within 20° (~ 1400 km) of
237 distance or less from the wave breaking episode found at day T_n , we assume that this event is an

238 extension of the RWB event found the previous day. Else, we infer that the RWB episode only
239 lasted for a day.

240 4.- Step 3 is repeated for the following days until we stop finding wave breaking events that
241 fulfill the condition specified in step 2.

242 5.- We save the same characteristics of the RWB events detailed in section 2.3 as well as the day
243 a RWB event was detected after the dissipation of a RWP, and how many days lasts the RWB
244 associated to a RWP.

245 In step 2, we search for RWB events in the area located between $X_f \pm 2000$ km because even if
246 X_f signals the center of the RWP, the packet has a certain longitudinal extension, and thus the
247 RWB event does not have to necessarily appear near X_f . Barnes and Hartmann (2012) considered
248 that RWB events that are within 2000 km of the geographical center of the RWB belong to the
249 same episode, hence, in this study we look for RWB events that are up to 2000 km of distance
250 from the area of dissipation of the RWPs. On the other hand, we chose to search for events a few
251 days after the end of the RWPs propagation because it is possible that before disappearing the
252 RWPs might be stationary for a few days. By examining the evolution and behavior of several
253 potential vorticity fields several days after the dissipation of a RWPs we chose an upper limit of
254 4 days.

255 Additionally, in step 3 we used a distance of 1400 km to search for the continuation of a RWB
256 episode, because using a longer distance can cause the algorithm to select a wrong wave
257 breaking event that is too far away from the original episode that is being tracked.

258 Figure 2 shows an example of the methodology followed to link RWPs with RWB events.

259 2.5 Linking atmospheric blocking to large-scale Rossby wave breaking events

260 Lastly, we compared the proportion of large-scale RWB events that are present nearby the
261 development of an atmospheric blocking event. In order to detect the occurrence of atmospheric
262 blocking events, we use the methodology of Tibaldi and Moldenti (1989), but modified to
263 consider a range of latitudes in the Southern Hemisphere following Mendes *et al.*, (2011). This
264 technique measures two geopotential height meridional gradients from a central latitude, one to
265 the north (GHGN) and another one to the south (GHGS) by using expressions 1 and 2.

$$266 (1) \text{ GHGN} = (Z(\lambda, \theta_1) - Z(\lambda, \theta_N)) / (|\theta_1 - \theta_N|)$$

$$267 (2) \text{ GHGS} = (Z(\lambda, \theta_S) - Z(\lambda, \theta_2)) / (|\theta_S - \theta_2|)$$

268 Where

$$269 \theta_N = 40^\circ\text{S} + \Delta$$

$$270 \theta_2 = 50^\circ\text{S} + \Delta$$

271 $\theta_1 = 55^\circ\text{S} + \Delta$

272 $\theta_s = 65^\circ\text{S} + \Delta$

273 $Z(\lambda, \theta)$ is the geopotential height at 500 hPa in a latitude θ and longitude λ , and Δ belongs to the
274 set $\{-10, -7.5, -5, -2.5, 0, 2.5, 5, 7.5, 10\}$. If on a specific day, at a given longitude λ ,
275 $\text{GHGN} > 0$ and $\text{GHGS} < -10$ m/degree of latitude for, at least, one value of Δ , the longitude is
276 considered to be “blocked”. Note that, we measure GHGN and GHGS using slightly different
277 expressions from Mendes *et al.*, (2011). The definition chosen here implies a stronger
278 requirement on the blocked longitudes than the one considered in the latter study.

279 Once instantaneous, local, blocked conditions have been identified, additional persistence and
280 spatial extension requirements must be imposed to define atmospheric blocking events. Various
281 thresholds have been used in the literature. Patterson *et al.*, (2019) define an atmospheric
282 blocking event when they detect a blocked longitudinal sector covering, at least, 11° and when
283 this condition persists for a minimum of 4 days in the atmosphere. Mendes *et al.*, (2011), use a
284 minimum spatial extent of 7.5° in longitude and persistence of 5 days. In our study, we registered
285 events that have a minimum longitudinal extension of $7.5, 10, 12.5$ and 15° and display a
286 minimum lifespan of 4-5 days, measuring the longitude of detection, lifetime and zonal
287 extension of the blocks. This is done in order to assess whether the proportion of atmospheric
288 blocks that might be linked to RWB is sensitive to the blocking conditions. Hence, events that
289 last at least 4 days with a longitudinal extension of 7.5° are most frequent and represent blocking-
290 like situations, that is, the persistent reversal of the westerly wind flow that are not sufficiently
291 extensive to be considered as a blocking event, whereas those that last more than 5 days and have
292 a zonal extension of at least 15° are considered the strongest blocks of the dataset.

293 In section 5, we first verify that our algorithm works as intended by measuring the frequency of
294 occurrence and areas of formation of blocking events in our period of study, comparing the
295 results to those obtained in Mendes *et al.*, (2011). We then study the potential links between
296 large-scale RWB events and blocking events by identifying the events which occur on the same
297 day and such that their respective geographical center are separated by a maximum of 2000 km.
298 The fulfillment of the latter conditions ensures that the RWB event is present near the
299 development of the atmospheric block. Lastly, we determine how many of the RWB events that
300 occur near an atmospheric block are associated to propagating RWPs. This analysis assesses the
301 proportion of atmospheric blocks that are associated to large-scale RWB activity, and whether
302 RWB activity linked to propagating RWPs is directly linked to the development of atmospheric
303 blocking events.

304 **3 Rossby wave breaking events and their relationship to Rossby Wave Packets**

305 3.1 Verification of Rossby Wave Breaking algorithm

306 The analysis of RWB events during the December-March season between 1979-2008 detected a
307 total of 659 RWB events in December, 470 in January, 413 in February and 581 events in March.
308 As for the orientation of the RWB events, 22% of the total wave breaking activity belongs to
309 cyclonic RWB, and the rest to anticyclonic RWB.

310 Figure 3 shows the longitudinal distribution of RWB frequency of occurrence. The maximum
311 RWB activity occurs in the western Pacific (between 140-200° E), and the lowest activity is
312 located near 0°E. These results indicate that RWB is weakest at the jet entrance in the Atlantic
313 basin, and largest at the jet exit, consistent with the fact that RWPs activity occurs in the
314 Atlantic-Indian basin where the strong jet acts as waveguide (Pérez *et al.*, 2021).

315 Additionally, figure 4 shows that the main area of anticyclonic RWB detection is located in the
316 western Pacific, as reported by Ndarana and Waugh (2010b). Nonetheless, we also observe two
317 secondary areas of maximum anticyclonic RWB activity, one located in the Indian Ocean and
318 the second in the eastern Pacific-western Atlantic. The latter is in agreement with Ndarana and
319 Waugh (2010b), but these authors found very little anticyclonic RWB activity in the Indian
320 Ocean during December-February. Nonetheless, Ndarana and Waugh (2010b) found significant
321 RWB activity in that region during March-May, suggesting that the differences with our results
322 are explained because of our consideration of March in the summer season. Thus, overall our
323 results are close to those observed in Ndarana and Waugh (2010b), providing a verification of
324 our RWB algorithm. It is worth pointing out that in our case the areas of RWB frequency have
325 wider meridional extension than those found in Ndarana and Waugh (2010b), because our
326 algorithm registers the whole latitudinal area where the overturning potential vorticity is
327 detected.

328 3.2 Characteristics of Rossby Wave Breaking after Rossby Wave Packet propagation

329 For the Southern Hemisphere summertime during 1979-2021, a total of 1256 RWPs were found,
330 which corresponds to around 30 per season. Moreover, 141 were LLRWPs, that is about 11% of
331 the total RWPs. From the 141 LLRWPs, 45% have associated large-scale RWB, whereas for the
332 SLRWPs (1115 cases) this proportion is close to 39%. In both cases RWB events show
333 anticyclonic shear: 79% (76%) of the RWB episodes detected after the propagation of a LLRWP
334 (SLRWP) show anticyclonic RWB.

335 Figure 5 displays the frequency of occurrence of RWB events as a function of longitude that
336 happened after the end of a LLRWPs/SLRWPs. When we focus on the RWB events linked to the
337 end of LLRWPs propagation, (figure 5a), we observe that the distribution of these events is
338 displaced eastward. As Pérez *et al.*, (2021) showed, LLRWPs tend to last longer and propagate
339 further into the western Pacific due to an extension of the jet wave guide modulated by the SAM.

340 On the other hand, most of the wave breaking events that appear after the dissipation of
341 SLRWPs, (figure 5b), tend to occur between 120-180°E, which corresponds to the Indian-
342 western Pacific sector. This is similar to the results obtained in previous studies (Ndarana and
343 Waugh 2010 a,b). The results found here are consistent with these results, such that an extended
344 jet stream allows LLRWPs to propagate further east and break in the Pacific ocean, instead of in
345 the eastern Indian ocean sector. Thus, RWB events associated with LLRWPs tend to occur in the
346 middle-eastern Pacific basin, which could imply that long-lived packets might be precursors of
347 weather regime transitions affecting conditions in South America.

348 Figure 6 shows temporal and spatial characteristics of the RWB events detected after the
349 dissipation of LLRWPs and SLRWPs. In figure 6a we display the number of days that pass until
350 a RWB event is detected after the dissipation of a RWP. The two distributions are similar, that is,
351 most of the RWB events occur the same or the next day after the RWP dissipation, although we
352 observe more dispersion in the LLRWPs distribution. Additionally, figure 6b shows the lifespan
353 of the RWB events, indicating that most of the RWB events last between 1-2 days, and that there
354 are no significant differences between both distributions. Nonetheless, when we compare the
355 zonal extension of the wave breaking events, (figure 6c), RWB events that occur after the
356 propagation of SLRWPs cover larger longitudinal extensions compared to those observed after
357 LLRWPs. RWB events linked to LLRWPs show a median longitudinal extension of 22°, and a
358 interquartile range of 12°, whereas RWB associated to SLRWPs have a median of 26.5° and
359 display an interquartile range of 15°. A Kruskal-Wallis test applied to the datasets of figure 6c,
360 indicates that the distributions are significantly different, at 5% level of significance.

361 Hence, these results suggest that RWB events caused by SLRWPs cover larger longitudinal
362 extensions of the atmosphere compared to those produced by LLRWPs. Nonetheless, neither
363 LLRWPs or SLRWPs seem to be directly related to atmospheric blocking development because,
364 even if the associated RWB events have similar spatial scales to a blocking event, they tend to
365 last only about 1-2 days, too short to lead to blocking (see also section 5).

366 **4 Interannual variability of Rossby Wave Breaking events associated to LLRWPs/SLRWPs**

367 The interannual variability in the occurrence of RWB associated to LLRWPs and SLRWPs is
368 shown in figure 7. Both time series show large year-to-year variability. In the case of LLRWPs,
369 the number of annual RWB events range from 0 to 11, while for SLRWPs it ranges from 6 to 32.
370 During certain periods the frequency of occurrence of RWB associated to the LLRWPs and
371 SLRWPs seem to be out of phase, but no significant correlation has been found between the two
372 time series.

373 Figure 8 shows the temporal evolution of the RWB events linked to LLRWPs together with the
374 SAM/ENSO indices, this is, the Antarctic Oscillation Index for SAM and the Oceanic Niño
375 Index for ENSO. A correlation analysis indicates that there is no linear relationship between the
376 number of RWB events linked to the dissipation of LLRWPs with SAM or ENSO. It is also

377 worth noting that one reason that can influence the results is that we have several years without
378 RWB activity linked to LLRWPs, which can increase the difficulty of finding significant
379 correlation between the timeseries of RWB events linked to LLRWPs and SAM or ENSO
380 activity.

381 On the other hand, the interannual variability of RWB events linked to SLRWPs is correlated
382 with SAM/ENSO indices (Figure 9). Years with positive SAM have a higher frequency of
383 occurrence of RWB linked to SLRWPs, and the opposite occurs in years with negative SAM.
384 This is reflected in a Pearson correlation coefficient value of 0.25 between the Antarctic
385 Oscillation Index and the RWB events linked to SLRWPs, which is statistically significant at
386 10% level (using Student t-test). Moreover, a similar analysis indicates that the correlation
387 between the Oceanic Niño Index and RWB events linked to SLRWPs is -0.35, statistically
388 significant at 5% level. Thus, La Niña years tend to favor the development of RWB events,
389 whereas El Niño years do the opposite. In agreement, Wang and Magnusdottir (2010) and Gong
390 *et al.*, (2010) concluded that RWB in the tropical/subtropical Pacific is increased during La Niña
391 events, and this was associated to a strong local decrease in the zonal wind. At the same time
392 Barreiro (2017) found that El Niño events tend to favor the RWPs propagation. Therefore, El
393 Niño seems to induce large scale background conditions that favor the propagation of RWPs and,
394 by extension, diminishes the occurrence of RWB, whereas the wind flow decrease during La
395 Niña disfavors the propagation of RWPs and propitiates the occurrence of RWB events.

396 **5 Link between atmospheric blocking and large-scale Rossby Wave Breaking**

397 Results of section 3.2 suggest that the link between RWB associated with RWPs and blocking is
398 not obvious because these RWB events tend to last 1 or 2 days. Here we look further into the
399 relationship between RWB and blockings.

400 Table 1 shows the number of blocking events found as a function of the persistence and
401 longitudinal extension considered. For the less restrictive criteria (blocks that last at least 4 days
402 and with a minimum longitudinal extension of 7.5°) there are 263 events between 1979-2020
403 summertime, which corresponds to around 6 blocking events per season. This large number of
404 events reflects the fact that these criteria cause the finding of more blocking-like situations than
405 atmospheric blocks. On the other hand, for the most intense blocks (lifespan of 5 or more days
406 and with a minimum extension of 15°) there are 55 events, this is, a mean of 1.3 events per year.
407 As expected, we observe a decrease in blocking events as the conditions become more
408 restrictive.

409 It is worth mentioning that we find a mean of 3 atmospheric block events per year when we
410 follow the criteria of Mendes *et al.*, (2011), which is similar to the number they found (between
411 2.9-3.1 events per year).

412 In addition, when we focus on the detection areas of blockings, we find that near 50% of the
413 events appear at the central-western Pacific basin (181-240°E) independently of the zonal
414 extension and persistence of the event. On the other hand, there is a secondary area of blocking
415 development in the eastern Indian basin (121-180°E), where we find around 23-38% of the
416 blocking events, showing the highest (lowest) values during the strongest (weakest) blocking
417 events. Oppositely, we barely detect any blocking in the western south-Atlantic (300-359°E) or
418 the central Indian basin (0-60°E). These results are summarized in table 2 and are in accordance
419 with the observations in Hendes *et al.*, (2011).

420 The search for large-scale RWB associated to the formation of an atmospheric block reveals that
421 the latter appear close to a RWB event between 15-18% of the times independently of the
422 strength and stability of the block (not shown). Also, in agreement with the results of section 3.2,
423 we only found RWB linked to propagating RWPs near the development of an atmospheric block
424 around 3-6% of the times, and it does not seem to depend on the intensity and stability of the
425 block.

426 To summarize, RWB events are present in the atmosphere around 1 out of 5 times an
427 atmospheric block is detected in the atmosphere, but these RWB events do not seem to be related
428 with the propagating RWPs. Thus, propagating RWPs do not seem to be directly linked to the
429 development of atmospheric blocks. We recall that here we described propagating RWPs as those
430 with speed between 15-45°/day eastward, a zonal number between 4-12 days, and lifespan larger
431 than three days.

432 **6 Summary and conclusions**

433 Rossby Wave Breaking events are atmospheric perturbations that interfere in the wind and
434 energy flow, and under certain circumstances they can cause an atmospheric block, leading to the
435 development of heatwaves or droughts. In this work, an algorithm to track overturning regions of
436 potential vorticity was developed in order to identify Rossby Wave breaking areas that are linked
437 to the dissipation of transient Rossby Wave Packets.

438 We found that both long-lived Rossby Wave Packets and short-lived Rossby Wave packets tend
439 to show wave breaking events around 40% of the time, although this number is slightly higher
440 for long-lived packets. Rossby Wave breaking events that occur preceded by long-lived Rossby
441 Wave Packets tend to manifest at the center-eastern part of the Pacific basin, and are less zonally
442 extended compared to the wave breaking events associated with the rest of the packets.
443 Therefore, changes in weather regime conditions caused by wave breaking events that are linked
444 to long-lived Rossby Wave Packets are more likely to occur at the south of South America.
445 Moreover, wave breaking events linked to Rossby Wave Packets tend to last between 1-2 days in
446 the atmosphere for both long-lived and short-medium lived packets. Thus, wave breaking events
447 produced by propagating RWPs do not seem to be directly linked to the development of
448 atmospheric blocks.

449 Previous studies have found that negative SAM years are characterized by a larger number of
450 long-lived Rossby Wave Packets due to the extension of the Atlantic-Indian basin jet wave guide
451 into the Pacific (Pérez *et al.*, 2021). Here we report that the frequency of wave breaking linked to
452 long-lived Rossby Wave packets do not seem to be affected by SAM nor ENSO. On the
453 contrary, positive SAM conditions and La Niña events favor the development of wave breaking
454 episodes after the propagation of short-lived RWPs. Pérez *et al.*, (2021) concluded that the
455 frequency of occurrence of long-lived Rossby Wave packets is negatively correlated with the
456 number of short-lived Rossby Wave Packets. Thus, years with positive SAM conditions cause a
457 decrease in the number of long-lived Rossby Wave Packets and an increase of short-lived
458 packets. Consequently, the amount of Rossby Wave breaking events linked to Rossby Wave
459 Packets is expected to increase in years with positive SAM events. In addition, results also
460 suggest that RWB events are more common during years with La Niña.

461 Finally, we assess whether Rossby Wave Breaking events appear near the development of
462 atmospheric blocks, and found that around 1 out of 5 times a blocking event develops, a Rossby
463 Wave Breaking event is present. However, Rossby Wave Breaking linked to propagating Rossby
464 Wave Packets do not seem to be associated to atmosphere blocking development. Therefore,
465 blocking event development during southern hemisphere summertime might be linked to other
466 atmospheric perturbations not considered in this study such as stationary Rossby Wave packets,
467 propagating wave packets with very low wavenumber (1-3), or they might be triggered by other
468 atmospheric processes.

469 **Data availability Statement**

470 ERA5 reanalysis data are freely available in the Copernicus Climate Data Store
471 <https://cds.climate.copernicus.eu/>, whereas ENSO and SAM indexes are available at
472 <https://origin.cpc.ncep.noaa.gov/>. The wind envelope amplitude of the RWPs used in this study
473 is publicly available at <https://doi.org/10.5281/zenodo.5714192>, and a script describing how to
474 obtain wind envelope data from meridional wind speed at
475 <https://doi.org/10.5281/zenodo.5724656>.

476 **Acknowledgments**

477 This project has received funding from the European Union's Horizon 2020 research and
478 innovation programme under the Marie Skłodowska-Curie grant agreement No 813844 (ITN
479 CAFÉ). NE, CL and EHG acknowledge grant PID2021-123352OB-C32 funded by MCIN/AEI/
480 10.13039/501100011033 FEDER/UE.

481

482

483 **References**

- 484 Altenhoff, M, A., Martius, O., Croci-Maspoli, M.,Schwierz, C & Davies,C,H. (2008) Linkage of atmospheric blocking and
 485 synoptic-scale Rossby waves: a climatological analysis, *Tellus A: Dynamic Meteorology and Oceanography*, 60(5), 1053-1063,
 486 <https://doi.org/10.1111/j.1600-0870.2008.00354.x>
- 487 Barnes, A, E and Hartmann, L,D. (2012) Detection of Rossby wave breaking and its response to shifts of the midlatitude jet with
 488 climate change. *Journal of Geophysical Research*, 117(D9). <https://doi.org/10.1029/2012JD017469>
- 489 Berrisford, P., Hoskins, J, B and Tyrlis, E. (2007) Blocking and Rossby Wave Breaking on the Dynamical Tropopause in the
 490 Southern Hemisphere. *Journal of the Atmospheric Sciences*,64(8), 2881-2898. <https://doi.org/10.1175/JAS3984.1>
- 491 Chang, E. K. M. (1999) Characteristics of wave packets in the upper troposphere. Part II: Seasonal and hemispheric variations.
 492 *Journal of Atmospheric Sciences*, 56(11), 1729-1747. [https://doi.org/10.1175/1520-0469\(1999\)056<1729:COWPIT>2.0.CO;2](https://doi.org/10.1175/1520-0469(1999)056<1729:COWPIT>2.0.CO;2)
- 493 Chang, E. K. M., & D. B. Yu. (1999) Characteristics of wave packets in the upper troposphere. Part I:Northern Hemisphere
 494 winter. *Journal of Atmospheric Sciences*, 56(11), 1708-1728. [https://doi.org/10.1175/1520-0469\(1999\)056<1708:COWPIT>2.0.CO;2](https://doi.org/10.1175/1520-0469(1999)056<1708:COWPIT>2.0.CO;2)
- 495
- 496 Chang, E. K. M. (2000) Wave Packets and Life Cycles of Troughs in the Upper Troposphere: Examples from the Southern
 497 Hemisphere, Summer Season of 1984/1985. *Monthly Weather Reviewer*, 128(1), 25-50. [https://doi.org/10.1175/1520-0493\(2000\)128<0025:WPALCO>2.0.CO;2](https://doi.org/10.1175/1520-0493(2000)128<0025:WPALCO>2.0.CO;2)
- 498
- 499 Chang, E. K. M. (2005) The Impact of Wave Packets Propagating across Asia on Pacific Cyclone Development. *Monthly*
 500 *Weather Review*, Vol 133(7) 1998-2015. <https://doi.org/10.1175/MWR2953.1>
- 501 Gong, T., Feldstein, B. S., Luo, D. (2010) The Impact of ENSO on Wave Breaking and Southern Annular Mode Events.*Journal*
 502 *of the atmospheric Sciences*, 67(9), 2854-2870. <https://doi.org/10.1175/2010JAS3311.1>
- 503 Grazzini, F and Vitart F. (2015) Atmospheric predictability and Rossby wave packets. *International Journal. of the Royal .*
 504 *Meteorological. Society*, 141(692), 2793-2802. <https://doi.org/10.1002/qj.2564>
- 505 Hans, H., Bell, B., Berrisford, P., Hirahara, S., Horány, A.,Muñoz-Sabater, *et al.* (2020) The ERA5 global reanalysis. *Royal*
 506 *Meteorological Society*, 146(730), 1999-2049. <https://doi.org/10.1002/qj.3803>
- 507 Hitchman, H. M., and Huesmann,S,A. (2007) A seasonal clima-tology of Rossby wave breaking in the 320–2000-K layer.
 508 *J.Atmos. Sci.*, 64(6), 1922–1940. <https://doi.org/10.1175/JAS3927.1>
- 509 Holton, J. R., Haynes , H P., McIntyre, E. M., Douglass,R, A., Roodm. B., R and Pfister, L. (1995) Stratosphere–troposphere
 510 exchange. *Rev. Geophys.*, 33(4), 403–439. <https://doi.org/10.1029/95RG02097>
- 511 Hoskins,J,N., Ambrizzi, T. (1993) Rossby Wave Propoagation on a Realistic Longitudinally Varying Flow. *Journal of the*
 512 *Atmospheric Sciences*, 50(12). [https://doi.org/10.1175/1520-0469\(1993\)050<1661:RWPOAR>2.0.CO;2](https://doi.org/10.1175/1520-0469(1993)050<1661:RWPOAR>2.0.CO;2)

- 513 Hoskins J.B., McIntyre E.M., Robertson W.A. (1985) On the use and significance of isentropic potential vorticity maps. *Q. J. R.*
514 *Meteorol. Soc.* 111(470), 877–946. <https://doi.org/10.1002/qj.49711147002>
- 515 Masato, G., Hoskins, J.B., Woollings, T. (2011) Wave breaking characteristics of mid-latitude blocking. *Quarterly Journal of the*
516 *Royal Meteorological Society*, 138(666), 1285-1296. <https://doi.org/10.1002/qj.990>
- 517 Masato, G., Hoskins, J.B., Woollings, T. (2013) Wave-Breaking Characteristics of Northern Hemisphere Winter Blocking: A Two-
518 Dimensional Approach. *Journal of Climate*, 26(13), 4535-4549. <https://doi.org/10.1175/JCLI-D-12-00240.1>
- 519 Mendes, M. C. D., Cavalcanti, I. F., & Herdies, D. L. (2011) Southern Hemisphere atmospheric blocking diagnostic by ECMWF
520 and NCEP/NCAR data. *Revista Brasileira de Meteorologia*, 27(3), 263-271. <https://doi.org/10.1590/S0102-77862012000300001>
- 521 Michel, C and Rivi re, G (2011) The Link between Rossby Wave Breaking and Weather Regime Transitions. *Journal of The*
522 *Atmospheric Sciences*, 68(8), 1730-1748. <https://doi.org/10.1175/2011JAS3635.1>
- 523 McIntyre, E. M., and Palmer, T.N (1983) Breaking planetary waves in the stratosphere. *Nature*, 305, 593–600.
524 <https://doi.org/10.1038/305593a0>
- 525 McIntyre, E. M and Palmer, T.N., Palmer, (1984) The “surf zone” in the stratosphere. *J. Atmos. Terr. Phys.*, 46(9), 825–839.
526 [https://doi.org/10.1016/0021-9169\(84\)90063-1](https://doi.org/10.1016/0021-9169(84)90063-1)
- 527 Ndarana, T and Waugh, D., (2010a) The link between cut-off lows and Rossby wave breaking in the Southern Hemisphere. *Q.J.R*
528 *Meteorol. Soc.* 136(649), 869-885. <https://doi.org/10.1002/qj.627>
- 529 Ndarana, T and Waugh, W,D (2010b) A climatology of Rossby Wave Breaking on the Southern Hemisphere Tropopause.
530 *Journal of the Atmospheric Sciences*, Vol 68, 798-811. <https://doi.org/10.1175/2010JAS3460.1>
- 531 O’Brien L., & Reeder, J. M. (2017) Southern Hemisphere Summertime Rossby Waves and Weather in the Australian Region.
532 *Quarterly Journal of the Royal Meteorological Society*. 143(707), 2374-2388. <https://doi.org/10.1002/qj.3090>
- 533 Patterson, M., Bracegirdle, T., & Woollings, T. (2019) Southern Hemisphere atmospheric blocking CMIP5 and future changes in
534 the Australia-New Zealand sector. *Geophysical Research Letters*, 46(15), 9281–9290. <https://doi.org/10.1029/2019GL083264>
- 535 Peters, D., and Waugh, W, D. (1996) Influence of barotropic shear on the poleward advection of upper-tropospheric air. *J. Atmos.*
536 *Sc.* 53(21), 3013–3031. [https://doi.org/10.1175/1520-0469\(1996\)053<3013:OBSOT>2.0.CO;2](https://doi.org/10.1175/1520-0469(1996)053<3013:OBSOT>2.0.CO;2)
- 537 Peters, D., and Waugh, W, D. (2003) Rossby wave breaking in the Southern Hemisphere wintertime upper troposphere. *Mon.*
538 *Wea. Rev.*, 131(11), 2623–2634. [https://doi.org/10.1175/1520-0493\(2003\)131<2623:RWBITS>2.0.CO;2](https://doi.org/10.1175/1520-0493(2003)131<2623:RWBITS>2.0.CO;2)
- 539 P rez, I., Barreiro, M., & Masoller, C. (2021) ENSO and SAM influence on the generation of long episodes of Rossby Wave
540 Packets during Southern Hemisphere summer. *Journal of Geophysical Research: Atmospheres*, 126(24).e2021JD035467
541 <https://doi.org/10.1029/2021JD035467>
- 542 Rex, D. F. (1950) Blocking action in the middle troposphere and its effect upon regional climate. *Tellus*, 2(3), 196–211.
543 <https://doi.org/10.3402/tellusa.v2i4.8603>

- 544 Ryoo, J-M., Kaspi, Y., Waugh, W , D., Kiladis, N, G., Waliser, E, D., Fetzer, J, E and Jinwon, K. (2013) Impact of Rossby Wave
545 Breaking on U.S. West Coast Winter Precipitation during ENSO Events,*Journal of Climate*,26(17), 6360-6382.
546 <https://doi.org/10.1175/JCLI-D-12-00297.1>
- 547 Sagarra, R., & Barreiro, M. (2020) Characterization of extratropical waves during summer of the Southern Hemisphere.
548 *Meteorologica*, 45(2), 63-79. <https://hdl.handle.net/20.500.12008/33550>
- 549 Simmons, J. A., and Hoskins,J,B (1978) The life cycles of somenonlinear baroclinic waves. *J. Atmos. Sci.*, 35(3), 414–432.
550 [https://doi.org/10.1175/1520-0469\(1978\)035<0414:TLCOSN>2.0.CO;2](https://doi.org/10.1175/1520-0469(1978)035<0414:TLCOSN>2.0.CO;2)
- 551 Souders, B. M., Colle, A. B., & Chang, M. K. E. (2014a) The climatology and characteristics of Rossby Wave Packets using a
552 feature-based tracking technique. *Monthly Weather Review*, 142(10), 3528–3548. <https://doi.org/10.1175/MWR-D-13-00371.1>
- 553 Souders, B. M., Colle, A. B., & Chang, M. K. E. (2014b) A Description and Evaluation of an Automated Approach for Feature-
554 Based Tracking of Rossby Wave Packets. *Monthly Weather Review*, 142(10), 3505–3527. <https://doi.org/10.1175/MWR-D-13-00317.1>
555
- 556 Strong, C and Magnusdottir, G. (2008) Tropospheric Rossby Wave Breaking and the NAO/NAM, *Journal of the Atmospheric*
557 *Sciences*,65(9), 2861-2876 <https://doi.org/10.1175/2008JAS2632.1>
- 558 Tibaldi, S. and Molteni, F (1990) On the operational predictability of blocking. *Tellus A*, 42, 343-365.
559 <https://doi.org/10.1034/j.1600-0870.1990.t01-2-00003.x>
- 560 Thorncroft, D. C., Hoskins, J, B, and McIntyre,E,M (1993) Two paradigms of baroclinic-wave life-cycle behaviour. *Quart. J.*
561 *Roy. Meteor. Soc.*, 119(509), 17–55.<https://doi.org/10.1002/qj.49711950903>
- 562 Trenberth, E. K. (1981). Observed Southern Hemisphere Eddy Statistics at 500 mb: Frequency and Spatial Dependence. *Journal*
563 *of Atmospheric Science*, 38(12), 2585–2605. [https://doi.org/10.1175/1520-0469\(1981\)038<2585:OSHESA>2.0.CO;2](https://doi.org/10.1175/1520-0469(1981)038<2585:OSHESA>2.0.CO;2)
- 564 Wang, Y and Magnusdottir, G (2010) Tropospheric Rossby Wave Breaking and the SAM, 24(8), 2134-2146,
565 <https://doi.org/10.1175/2010JCLI4009.1>
- 566 Wiedenmann, M,J., Lupo,R,A., Mokhov, I, I and Tikhonova, A, E. (2002) *Journal of Climate*, 15(23), 3459-3473.
567 [https://doi.org/10.1175/1520-0442\(2002\)015<3459:TCOBAF>2.0.CO;2](https://doi.org/10.1175/1520-0442(2002)015<3459:TCOBAF>2.0.CO;2)
- 568 Wirth, V., Riemer, M., Chang, E, K, M., & Martius, O. (2018) Rossby Wave Packets on the Midlatitude waveguide- a review.
569 *Monthly Weather Review*, 146(7), 1965-2001. <https://doi.org/10.1175/MWR-D-16-0483.1>
- 570 Wirth, V. (2020) Waveguidability of idealized midlatitude jets and the limitations of ray tracing theory. *Weather Climate*
571 *Dynamics*, 1, 111–125. <https://doi.org/10.5194/wcd-1-111-202>
- 572 Woollings, T., Barriopedro, D., Methven, J., Son, S.-W., Martius, O., Harvey, B., et al. (2018) Blocking and its response to
573 climate change. *Current Climate Change Reports*, 4, 287–300. <https://doi.org/10.1007/s40641-018-0108-z>

574 Yeh, T. C. (1949) On energy dispersion in the atmosphere. *Journal of Meteorology*, 6(1), 1–16. [https://doi.org/10.1175/1520-0469\(1949\)006<0001:OEDITA>2.0.CO;2](https://doi.org/10.1175/1520-0469(1949)006<0001:OEDITA>2.0.CO;2)

576 Zheng, M., Chang, E. K., & Colle, B. A. (2013) Ensemble sensitivity tools for assessing extratropical cyclone intensity and track predictability. *Weather and forecasting*, 28(5), 1133-1156.. <https://doi.org/10.1175/WAF-D-12-00132.1>

578 **Tables**

	7.5° L	10°L	12.5°L	15°L
4d	263	212	168	123
	7.5°L	10°L	12.5°L	15°L
5d	142	107	79	55

579 **Table 1.** Number of blocking events found using different criteria, (d) refers to minimum
 580 lifespan in days and (L) the minimum longitudinal extension in degrees of the atmospheric
 581 blocks detected.

582

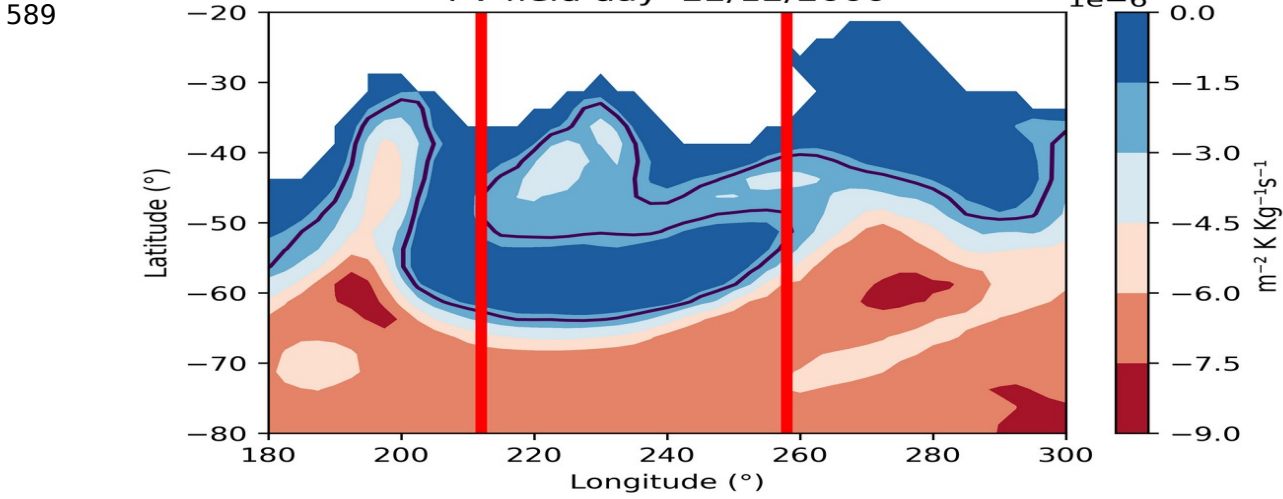
	Eastern South-Atlantic- western Indian basin (0- 60°E)	Central Indian basin (61-120°E)	Eastern Indian basin (121-180°E)	Western Pacific basin (181-240°E)	Eastern Pacific basin (241-300°E)	Western South- Atlantic (301-359°E)
4d 7.5° L	10	16	63	118	38	18
5d 15° L	1	2	20	27	4	1

583 **Table 2.** Number of summertime blocking events between 1979 and 2020 in the area of study for
 584 two blocking detection criteria: (d) refers to minimum lifespan of the event in days, and (L) to its
 585 minimum longitudinal extension in degrees.

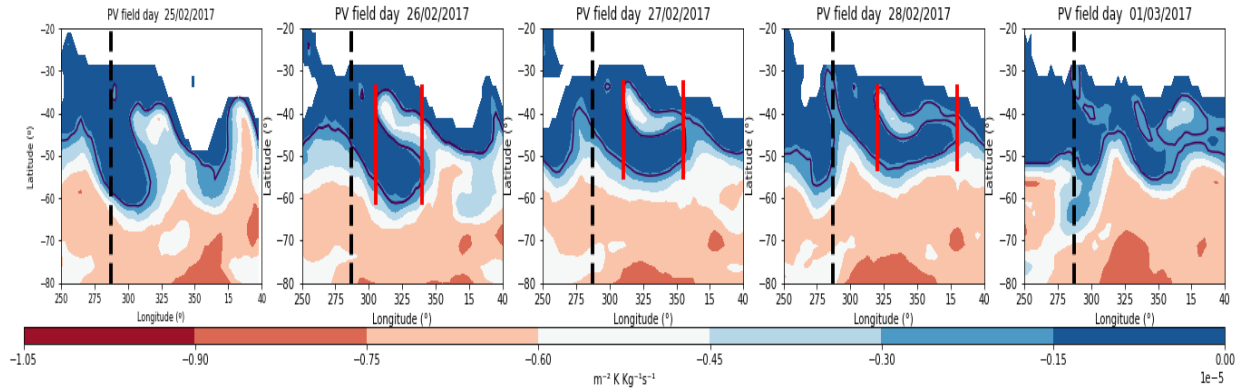
586

587

588 **Figures**

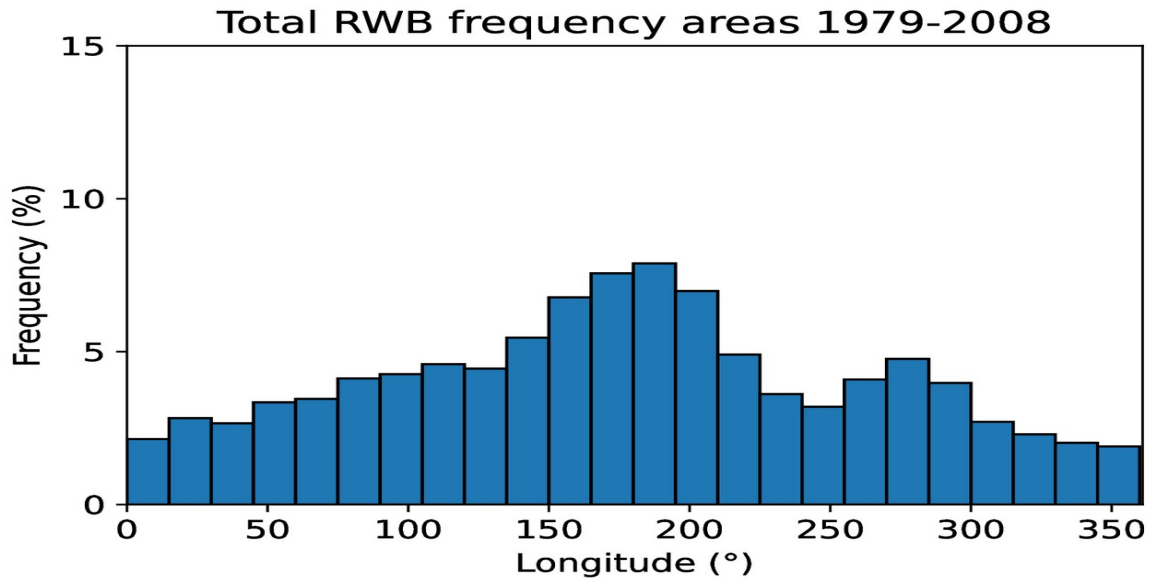


590 **Figure 1.** Potential vorticity fields following the 330°K isentropic isosurface during an anticyclonic RWB
 591 event detected on 22/12/2000. Red lines indicate the longitudinal section where the algorithm found the
 592 RWB event and the black line signals the location of the -2PVU line.

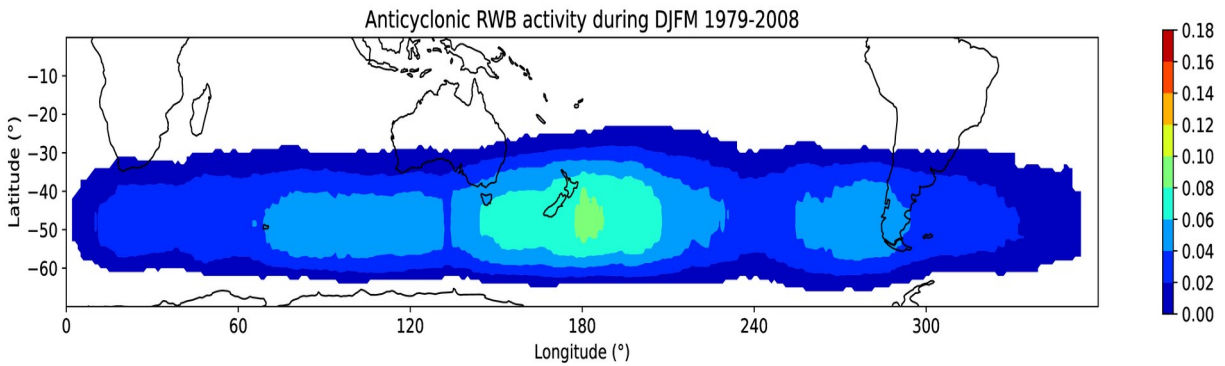


593 **Figure 2.** Potential vorticity fields following the 330°K isosurface between 25/02/2017-01/03/2017. The
 594 dashed black line shows the longitudinal section where a LLRWPs stopped its propagation at 25/02/2017,
 595 red lines indicate the area of RWB detected by the wave breaking algorithm and the black line signals the
 596 location of the -2PVU line.

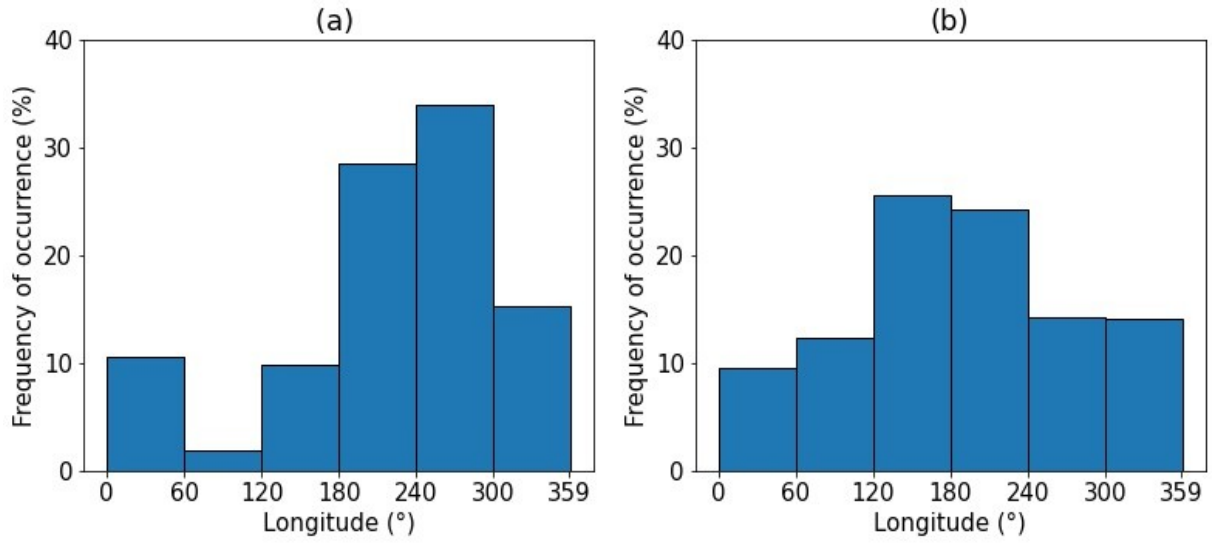
597



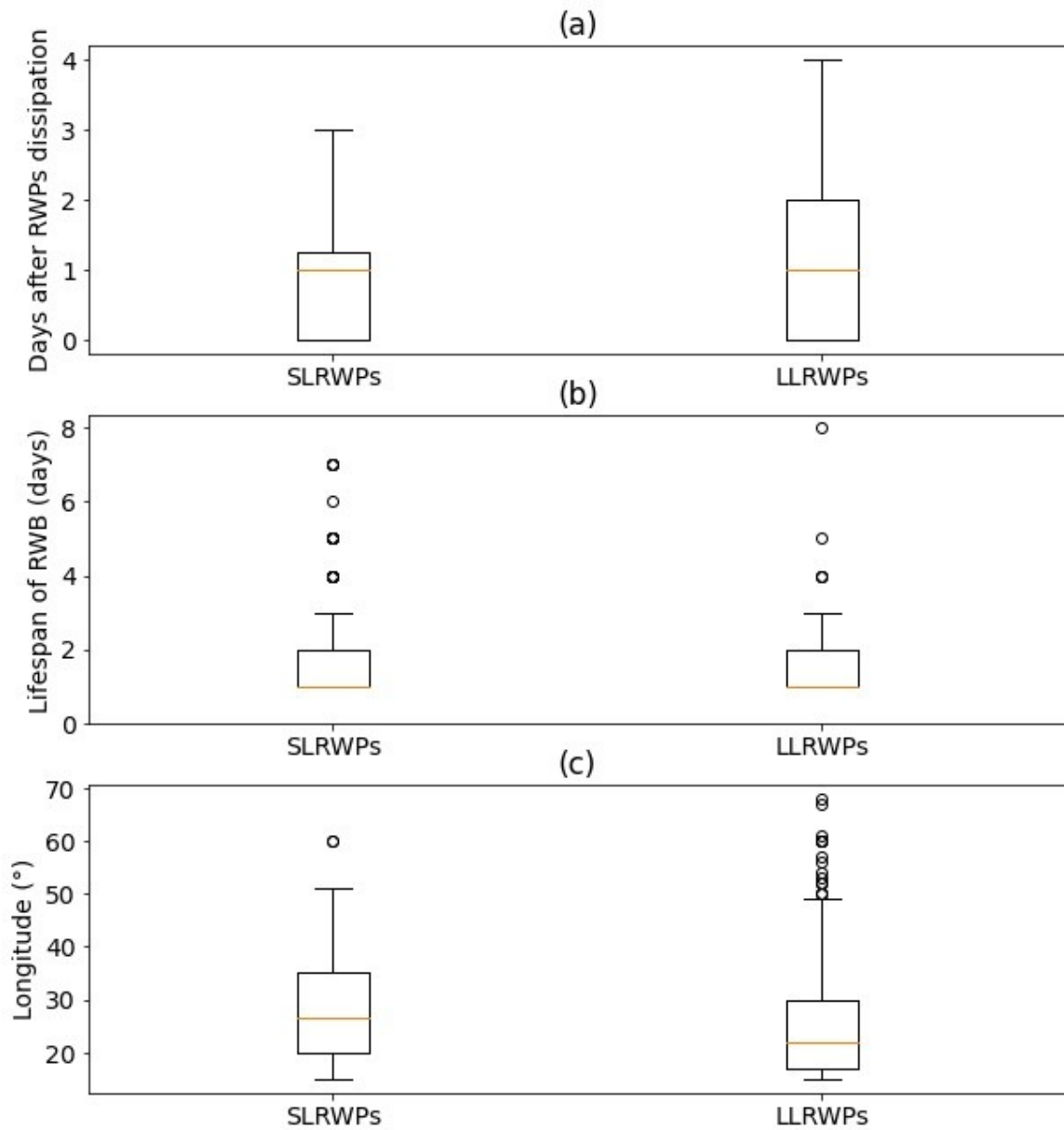
598 **Figure 3.** Frequency of RWB events found during summertime in the Southern Hemisphere between
599 1979-2008.



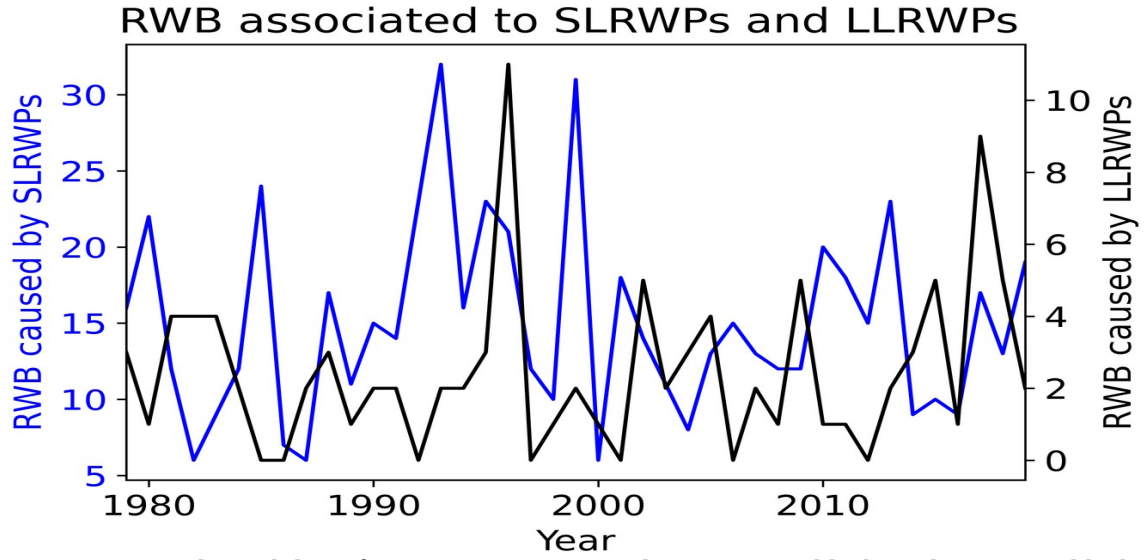
600 **Figure 4.** Anticyclonic RWB frequency found between 1979-2008. Colored areas show where RWB
601 episodes were detected.



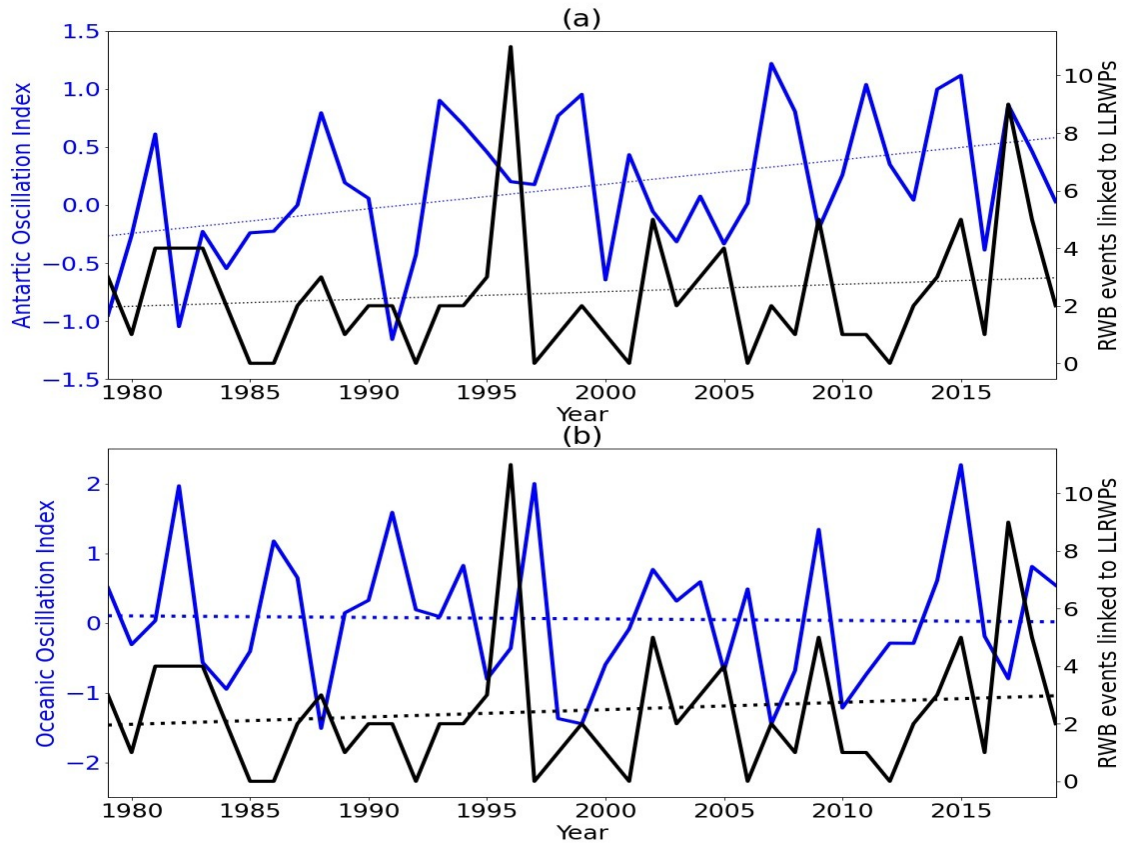
602 **Figure 5.** Relative frequency of occurrence of large-scale RWB associated to (a) LLRWPs and (b)
603 SLRWPs.



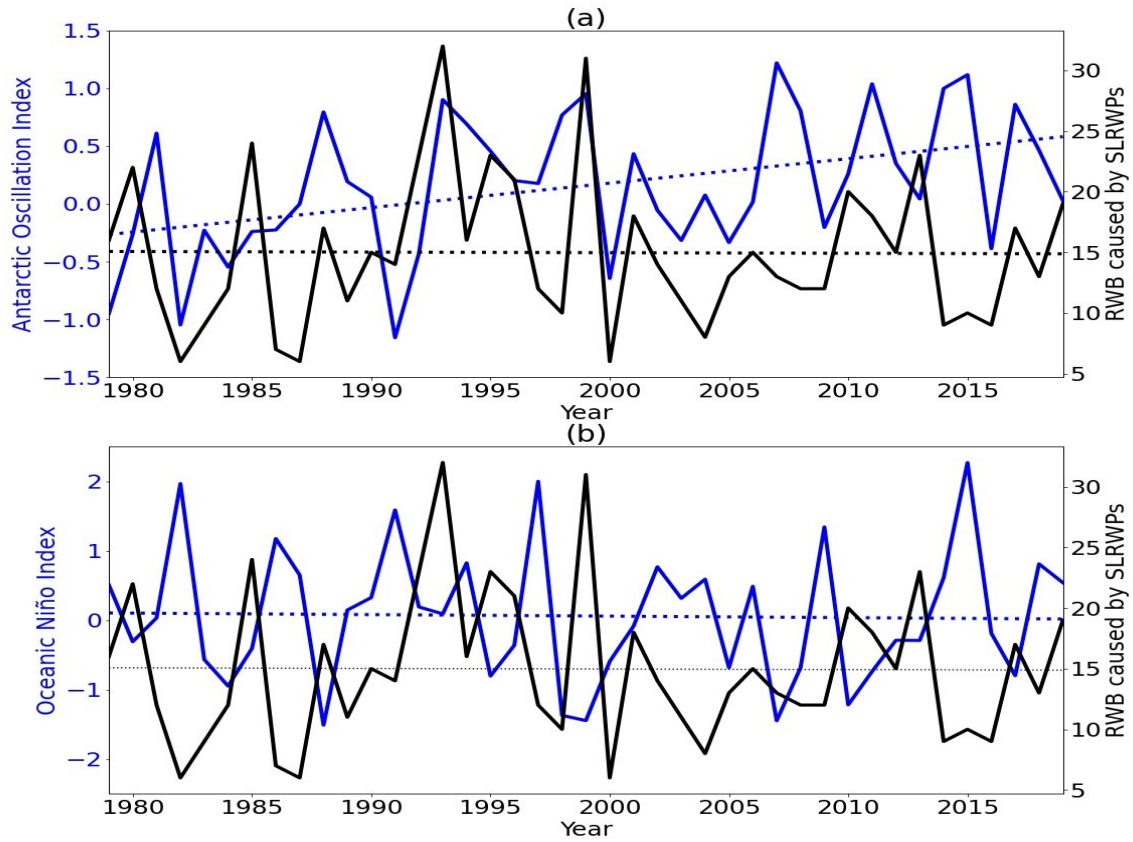
604 **Figure 6.** Boxplot distribution of several characteristics of RWB associated with LLRWPs and SLRWPs.
 605 Yellow lines in the boxplots signal the location of the median of the distribution. Upper figure (a) shows
 606 the day when a large-scale RWB event appears after the end of the RWPs propagation, middle figure (b)
 607 displays the mean lifespan of the RWB events, whereas the last figure shows the longitudinal extension of
 608 the RWB.



609 **Figure 7.** Interannual variability of RWB events associated to LLRWPs (black) and SLRWPs (black
610 lines).



612 **Figure 8.** Timeseries of annual RWB events associated to LLRWPs (black lines), against the temporal
 613 evolution of Oceanic Niño Index (a) and Antarctic Oscillation Index (b) during the period of study (blue
 614 lines). Dotted lines show the trend for each timeseries.



615 **Figure 9.** Timeseries of annual RWB events associated to SLRWPs (black lines), against the temporal
 616 evolution of Oceanic Niño Index (a) and Antarctic Oscillation Index (b) during the period of study (blue
 617 lines). Dotted lines show the trend for each timeseries.